



Biomechanical parameters of marram grass (*Calamagrostis arenaria*) for advanced modeling of dune vegetation

Viktoria Kosmalla¹, Oliver Lojek¹, Jana Carus², Kara Keimer¹, Lukas Ahrenbeck¹, Björn Mehrrens¹, David Schürenkamp¹, Boris Schröder^{2,3}, and Nils Goseberg^{1,4}

¹Technische Universität Braunschweig, Leichtweiß-Institute for Hydraulic Engineering and Water Resources; Division of Hydromechanics, Coastal and Ocean Engineering; Beethovenstraße 51a, 38106 Braunschweig, Germany

²Technische Universität Berlin, Institute of Ecology; Department of Plant Ecology; Rothenburgstraße 12, 12165 Berlin, Germany

³Berlin-Brandenburg Institute of Advanced Biodiversity Research; Altensteinstraße 6, 14195 Berlin, Germany

⁴Coastal Research Center; Joint Central Institution of Leibniz Universität Hannover and Technische Universität Braunschweig; Merkurstraße 14, 30419 Hannover, Germany

Correspondence: Viktoria Kosmalla (v.kosmalla@tu-braunschweig.de)

Abstract. This study investigates the biomechanical properties of marram grass (*Calamagrostis arenaria*, formerly *Ammophila arenaria*) over a 12-month period on the island of Spiekeroog, Germany, to enhance the modeling of coastal dune dynamics. The research reveals significant seasonal variations in the stiffness and Young's modulus of the vegetation, with higher values observed in winter, crucial for understanding dune erosion processes, and increased flexibility and density in summer, which are important for dune accretion. The findings emphasize the importance of incorporating seasonally adjusted parameters into models, particularly accounting for the increased horizontal density, the presence of flower stems in summer, and the longer leaf lengths in winter. The study also highlights the differentiation among plant parts, with flower stems providing the highest structural support due to their greater stiffness, while leaves contribute more to flexibility and dynamic responses. Interestingly, the minimal differences between green and brown leaves suggest that these can be treated similarly in modeling efforts, allowing for a simplified representation without compromising accuracy. Additionally, the study found no consistent evidence that wind exposure significantly affects the biomechanical properties of marram grass, suggesting that wind influence may not need to be factored into biomechanical models. The results also demonstrate that the biomechanical properties of marram grass are broadly transferable between fixed and dynamic dune systems, supporting the application of these findings across various coastal environments. The key outcome of this research is the detailed compilation of the biomechanical traits of marram grass's aboveground vegetation, reflecting the seasonal dynamics found in dune processes, which will serve as a valuable resource for future modeling efforts of dune vegetation and their surrogates.

1 Introduction

Coastal dunes occur worldwide and belong to the most dynamic ecosystems on Earth. Their morphology is governed by an intricate interplay between physical and biological processes (Hesp, 2002; Hacker et al., 2012; Zarnetske et al., 2015; Stryppen et al., 2019). Sufficient sediment supply and strong onshore winds, together with pioneer vegetation, create a constantly



changing topography with dunes often reaching heights of tens of meters (Hacker et al., 2012; Duarte et al., 2013; Strypsteen et al., 2019; Mehrtens et al., 2023). After reaching a certain height, coastal dunes act as natural barriers, protecting inland areas from the impacts of storm tides by mitigating increased water levels and wave heights. This natural defense is crucial for safeguarding people, infrastructure, and the economy from flooding and related damages (Martínez and Psuty, 2004; Feagin et al., 2015; Ruggiero et al., 2018). Besides the economic value for coastal protection and tourism, coastal dunes also represent an important ecosystem with high ecological value regarding freshwater provision, biodiversity conservation, providing habitat for coastal vegetation as well as animals, especially nesting seabirds (Martínez and Psuty, 2004; Everard et al., 2010; Barbier et al., 2011; Röper et al., 2013; Ruggiero et al., 2018). The dynamic interactions between physical and biological processes result in high spatio-temporal complexity within dune systems (de Vries et al., 2012). Understanding the dynamics of dune erosion and accretion is essential, as these processes determine the safety level of coastal dunes against hinterland flooding due to storm surges (González-Villanueva et al., 2023), forming the basis for their integration as ecosystem-based coastal defense measures (de Vries et al., 2012; Feagin et al., 2015; de Battisti, 2021). Both short-term changes from individual storm events and long-term trends influenced by sea level rise, sediment supply, human activity, and the stabilizing effects of vegetation (Keijzers et al., 2016; Gao et al., 2020; Hovenga et al., 2021; González-Villanueva et al., 2023) are crucial for accurately assessing and managing the protective functions of coastal dunes (Keijzers et al., 2016; Gao et al., 2020; Farrell et al., 2023; Husemann et al., 2024).

One of the greatest challenges of this century pertains to deepen the understanding of and to develop adaptation measures against the vicissitude caused by climate change regarding coastal protection levels (sea level, storm frequency) and biodiversity (Dangendorf et al., 2019). The advantages of dunes over engineered hard structures (e.g., dikes and sea-walls) lie in their ability to form and stabilize dynamically through natural processes, such as aeolian sediment transport and vegetation growth. Furthermore, the dynamic processes of dune erosion and accretion lead to the assumption that by vertical growth (van Gent et al., 2008; van IJendoorn et al., 2021; Mehrtens et al., 2022, 2023) or landward migration, dunes can withstand sea level rise through adaptation under favorable conditions. Nowadays, sand nourishments are frequently used to artificially supply sediment for dune growth (Staudt et al., 2021); this way, dune systems are enabled to re-establish their former shape or geometry after storm damage (Keijzers et al., 2015). With this dynamic dune management, the natural processes governed by sediment supply, aeolian transport rates, and the vegetation cover are used exclusively for dune reconstruction (Keijzers et al., 2015). However, nature-based solutions (Nbs) in coastal protection are nowadays thought to serve the demands for both coastal protection and biodiversity preservation. Therefore, an enhanced understanding of the natural processes supports the integration of coastal protection measures and concepts. Furthermore, climate change also has an impact on the dune vegetation itself and may lead to alterations in species distribution and traits (Carter, 1991; Duarte et al., 2013; Gao et al., 2020; de Battisti, 2021; Biel and Hacker, 2021). Carter (1991), e.g., stated that species tolerant to higher temperatures, drought, and sand burial may become more dominant in the future. The enhanced understanding of vegetation development and characteristics is of particular importance, given that vegetation plays an essential role in the formation and evolution of coastal dunes and provides significant additional ecosystem services such as, e.g., carbon sequestration (Barbier et al., 2011). Numerous numerical models, e.g., DUBEVEG (Keijzers et al., 2016; Husemann et al., 2024), Aeolis (van Westen et al., 2024), or by implementations in



XBeach (Schweiger and Schuettrumpf, 2021), as well as physical models have been developed to simulate the interactions between vegetation, sand, wind, and water in dune environments. In physical experiments, vegetation is most often neglected (van Gent et al., 2007; Tomasicchio et al., 2011; Figlus et al., 2011; Mehrtens et al., 2024) or represented either by using real vegetation (Figlus et al., 2014; de Battisti and Griffin, 2020; Silva et al., 2016; Maximiliano-Cordova et al., 2019; Feagin et al., 2019) or simplistic mimics such as wooden dowels (Bryant et al., 2019; Kobayashi et al., 2013; Türker et al., 2019), presenting the challenge of either dealing with non-scalable materials or inadequately representing the actual properties of the vegetation (Garzon et al., 2021). Recent research in vegetation modeling for NbS in coastal protection has focused on improving the representation of plant physiology, morphology, and hydrology (Liu et al., 2021; Keimer et al., 2024). These models aim to capture the complex feedback mechanisms between vegetation and the environment, including the effects of plant traits on sediment transport, wind erosion, and water availability.

However, most biomechanical studies on coastal vegetation to date have focused on plant species commonly found in salt marshes, seagrass meadows, or mangrove forests. For instance, several studies have employed three-point bending tests for investigating the biomechanics of salt marsh vegetation and assessing seasonal differences (Rupprecht et al., 2015, 2017; Zhu et al., 2020; Liu et al., 2021; Paul et al., 2022; Keimer et al., 2023, 2024). In contrast, dune plants, such as European beachgrass, marram grass (*Calamagrostis arenaria*, formerly *Ammophila arenaria*, hereafter referred to as marram grass), have received much less attention, despite its critical role in dune stabilization and protection (Feagin et al., 2015; Davidson et al., 2020; de Battisti and Griffin, 2020). De Jong et al. (2014) explicitly emphasized the lack of research and highlighted the importance of studying vegetation development, particularly regarding density of cover and rooting depth; since then, little further research has appeared to fill the gap with better understanding the biomechanics of dune vegetation for facilitating modelling efforts.

Field data from the literature provides valuable insights into the characteristics of marram grass, though they can be difficult to interpret due to inconsistent terminology and often missing descriptions of methodologies. Histological examinations have been conducted by Andrade et al. (2021) and Chergui et al. (2017). A review by McGuirk et al. (2022) summarizes current knowledge on the role of vegetation in dune dynamics, including quantitative studies on marram grass by Hesp (1981, 1989), Hacker et al. (2012), Seabloom and Wiedemann (1994), Zarnetske et al. (2012), Biel et al. (2019), and Feagin et al. (2019). Key parameters examined include vegetation cover percentage (Bressolier and Thomas, 1977; Konlechner and Hilton, 2022; Chergui et al., 2017; Costas et al., 2024), aboveground and belowground biomass (de Battisti and Griffin, 2020; Mostow et al., 2021), tiller density (i.e., tillers per rhizome) (Hacker et al., 2012), plant density (Huiskes, 1979; Biel et al., 2019), stem density (Feagin et al., 2019), and stem and flower numbers per square meter (Seabloom and Wiedemann, 1994). Additionally, parameters such as stem length (Feagin et al., 2019; Mostow et al., 2021), and various height measurements (Hesp, 1981; Bressolier and Thomas, 1977; Mostow et al., 2021) have been reported. Feagin et al. (2019) explicitly addresses modeling and laboratory considerations of vegetation traits and provides additional information about marram grass, including stem diameter (3 ± 1 mm), leaves per square meter (1516 ± 8 leaves m^{-2}), leaves per stem (1 ± 3), leaf area (1605 ± 7 mm^2), and fine roots (288 ± 14 g m^{-2}). Growth heights range from 50 up to 100 cm (Bressolier and Thomas, 1977; Hesp, 1981). Stem height was reported to range up to 195 mm (Feagin et al., 2019), and stem lengths can reach up to 200 cm (Mostow et al., 2021). Plant density has been recorded up to 1000 tillers m^{-2} (Zarnetske et al., 2012), up to 200 tillers m^{-2} (Huiskes, 1979),



up to 556 tillers m^{-2} (Biel et al., 2019), 260 stems m^{-2} (Feagin et al., 2019), and approximately 203 stems m^{-2} , with about 30 flowers m^{-2} (Seabloom and Wiedemann, 1994). While these parameters are essential for developing accurate surrogate models, which we depict as non-withering, permanent laboratory replacement structures derived from in-situ characteristics of live plants, they primarily address geometric and external characteristics. To accurately model the physical interactions between vegetation and the environment, it is also crucial to understand mechanical plant traits. Studies such as Bouma et al. (2013) have demonstrated the importance of traits like shoot stiffness, shoot density, and shoot length in influencing the intensity and scale of interactions between organisms and their environment. However, there is currently limited knowledge on the mechanical properties of marram grass, such as flexibility and stiffness, which are vital for understanding plant biomechanics and their impact on dune stability and resilience to environmental stressors such as water or wind flow. These mechanical traits are crucial for accurately modeling how vegetation interacts with and mitigates the effects of these stressors on dune systems.

Vegetation in coastal ecosystems, such as salt marshes, exhibits marked seasonality in its traits. For example, during the summer, plant length and density significantly increase, while in the winter, the stiffness of the vegetation is greater and the outer diameter smaller (Koch et al., 2009; Vuik et al., 2017; Foster-Martinez et al., 2018; Keimer et al., 2024; Li et al., 2024). The effects of seasonality and vitality on vegetation traits can significantly impact their biomechanical properties, which in turn may influence the dune's stability and ability to withstand environmental stressors (Baas and Nield, 2010; de Jong et al., 2014; Biel and Hacker, 2021). Similarly, dune dynamics are also subject to seasonal variations. Dunes typically experience erosion during the winter and accretion during the summer, creating a seasonal cycle in dune morphology (Montreuil et al., 2013; Pye and Blott, 2016; Rader et al., 2018). These processes are driven by seasonal variations in wind and wave action, which shape the dune landscape. Although there is limited specific information on the seasonality of dune vegetation traits, it is known that marram grass has adapted to these dynamic processes. Marram grass requires regular sand burial for healthy growth, and without it, their growth and relative abundance decrease significantly (Maun, 1998; Bonte et al., 2021), indicating an "escape" mechanism against certain nematode species (van der Putten and Troelstra, 1990; Bonte et al., 2021). During the winter, the extensive root systems of these plants play a crucial role in stabilizing the dunes by enhancing the sediment's physical properties, such as porosity, shear strength, and slope stability, thus reducing erosion and preventing uprooting during storm surges (Davidson et al., 2020; Walker and Zinnert, 2022). In conclusion, the seasonality of vegetation traits combined with the seasonal dynamics of dune processes underscores the importance of incorporating seasonal variations in the study of dune vegetation properties for accurate modeling and understanding of the role of dune vegetation in coastal defense.

In addition, dune vegetation is subjected to varying external loads such as wind or hydrodynamics, which can influence plant growth and mechanical properties (Puijalon et al., 2005, 2011; Gardiner et al., 2016; Telewski, 2016; Du and Jiao, 2020; Kouhen et al., 2023). The mechanical stresses experienced by these plants can lead to different adaptive strategies. The reconfiguration of plants due to wind loads can be classified as either an avoidance strategy - minimizing frontal area - or a tolerance strategy - maximizing resistance to breakage: Plants following the avoidance strategy tends to have higher bending stiffness (Puijalon et al., 2011). Understanding these strategies is crucial for biomechanical characterization, as they influence how plants interact with environmental forces such as wind and waves. However, most studies on the impact of wind on biomechanical properties have focused on woody vegetation, such as trees, rather than on dune vegetation. The extent to which



these adaptive strategies apply to dune plants, such as marram grass, remains unclear. Given the significant role of wind in coastal environments, it is essential to investigate how dune vegetation responds to wind-induced mechanical stresses to better understand and model their biomechanical behavior.

Besides wind forces, soil characteristics also affect vegetation. Regarding dunes, the succession from younger white dunes to older gray or brown dunes alters the soil and thus the vegetation cover over the long-term (Isermann, 2011). Within white dunes, there are also differences, as they can be fixed or more mobile dunes (Isermann and Cordes, 1997). Whether these differences also have an effect on the biomechanical properties of the vegetation remains unclear.

By addressing the following research questions, this study aims to fill the aforementioned knowledge gaps by providing a comprehensive biomechanical characterization of marram grass, as the basis for accurate vegetation modeling in experiments, thus contributing to the understanding of dune vegetation dynamics and supporting the development of effective nature-based coastal protection strategies:

1. Are there significant seasonal variations in the biomechanical properties of dune vegetation that need to be considered separately for modeling accretion processes (in summer) and erosion processes (in winter)?
2. Do the different plant parts (sprouts, green leaves, brown leaves, flower stems) exhibit distinct biomechanical properties, or are they similar enough to be considered equivalent in biomechanical models of dune vegetation?
3. Does wind exposure (e.g., windward vs. leeward sides of dunes) or geographical exposition (e.g., north-west vs. south-east) affect the biomechanical traits of vegetation, and, if so, how should these factors be considered in biomechanical modeling?
4. How do biomechanical properties differ between vegetation in fixed, established dune systems and more dynamic dune systems, and how does this variation influence the accuracy and transferability of surrogate models in representing dune vegetation?

2 Methods

2.1 Study area

Field measurements were conducted on the East Frisian island Spiekeroog, which belongs to the North Sea barrier islands in Germany (see Figure 1a-b). The chain of barrier islands extends from Texel, the Netherlands to Fanø, Denmark, forming a landscape shaped by the littoral transport band driven by the counter-clockwise rotation of the tides into elongated west-east forms, further detailed by the interactions of waves, currents and wind (Pott, 1995). Located parallel to the coast, they isolate significant portions of the Wadden Sea from the open North Sea. From a geological perspective, these islands are very young, approximately 2000 years old, and were formed by an accumulation of Holocene marine sediments on a Pleistocene bed (Döring et al., 2021; Pollmann et al., 2018). By relocation of sandy sediments, pioneer dunes formed on the barrier islands and further evolved to dune chains reaching elevations of more than 20 metres above sea level (Pott, 1995). The side of the



dune chains averted from the ocean, the backbarrier, is protected from high-energy wave action of the open sea and, moreover, is dominated by mild sedimentation conditions, allowing accumulation of fine-grained marine sediments and the development of salt marshes (Bakker, 2014; Pollmann et al., 2018). The geomorphology of the North Sea barrier islands is characterized by the predominance of sands, a low-lying coastal region and high storm tide frequency (Pott, 1995). The wind conditions at Spiekeroog and the whole German North Sea are dominated by westerly winds, but in general wind directions are substantially fluctuating in this area (Hild et al., 1999; Röper et al., 2013; Deutscher Wetterdienst). Due to human activities, e.g., dredging, land reclamation, and a resulting alteration of the sand sedimentation processes, North Sea barrier islands are characterized by sand accumulation and a resulting narrow pointed island tip in the East. As a result, the geomorphology of the western and the younger eastern area of the barrier islands differ (Röper et al., 2013; Pollmann et al., 2018). Spiekeroog is located in 5 km distance from the German mainland and is part of the national park "Niedersächsisches Wattenmeer". As a major objective, the German national parks enable undisturbed natural dynamics and landscape processes; to that end, entering dunes is mostly prohibited. The eastern part of the island, the locally called *Ostplate* (germ. *Ost* = East, germ. *-plate* = flat), is highly protected and developed eastwards between 1650 and 1960, so that Spiekeroog continuously grew several kilometers to its present East-West length of approx. 10 km (Röper et al., 2013). The older western area is characterized by a well-developed, fixed dune system consisting of white, gray and brown dunes lined up from the beach in the North towards the center of the island (Isermann and Cordes, 1997; Pollmann et al., 2018). These dune types differ significantly with regard to soil type and predominant vegetation species (Boorman, 1988; Davis, 2011; Röper et al., 2013). The white dunes of the Spiekeroog island are mainly covered by European beach grass or marram grass (*Calamagrostis arenaria*, formerly *Ammophila arenaria*) (Pott, 1995; Röper et al., 2013; Pollmann et al., 2018), which is native to the Atlantic coast of Europe, but due to worldwide planting for dune stabilization, it now colonizes dunes between 32° and 60° latitude on both sides of the equator (Pickart, 2021).

We conducted dune surveys at two white dune sites on Spiekeroog island (see Fig. 1c). The first site, referred to as Dune Ridge, is a 20 m wide strip of a dune chain located at the southwestern shore of the island (53.753460° N, 7.674701° E) and is part of the fixed dune system of Spiekeroog Island (Isermann and Cordes, 1997). The second site, termed Cusp Dune, is a freestanding dune situated at the northern beach near the transition to the *Ostplate* (53.778793° N, 7.725181° E), surrounded by dune breaches, and characterized by younger and mobile dune systems (Isermann and Cordes, 1997).

These two sites have been selected due to their distinct environmental conditions. The Dune Ridge site is located in an area prone to erosion, necessitating regular reinforcement measures, and characterized by more narrow beaches. Approximately 800 m north of the Dune Ridge, significant sand nourishments are periodically required to maintain the beach-dune system, with the most recent effort involving 80,000 m³ of sand in 2023 (NLWKN, 14.07.2023). In contrast, the Cusp Dune is part of a more dynamic system, situated at the edge of the *Ostplate*, which is characterized by wide beaches, young morphological changes, and is influenced by the west-to-east sediment drift typical for the North Frisian islands. Being a freestanding dune, the Cusp Dune is surrounded by water during storm surges and thus exposed to both erosion and accretion processes from all directions.

Distinct study areas were established at each site based on dune morphology and wind exposure to investigate the impact on biomechanical vegetation traits. The Dune Ridge site (see Fig. 2) was divided into three zones based on wind exposure:

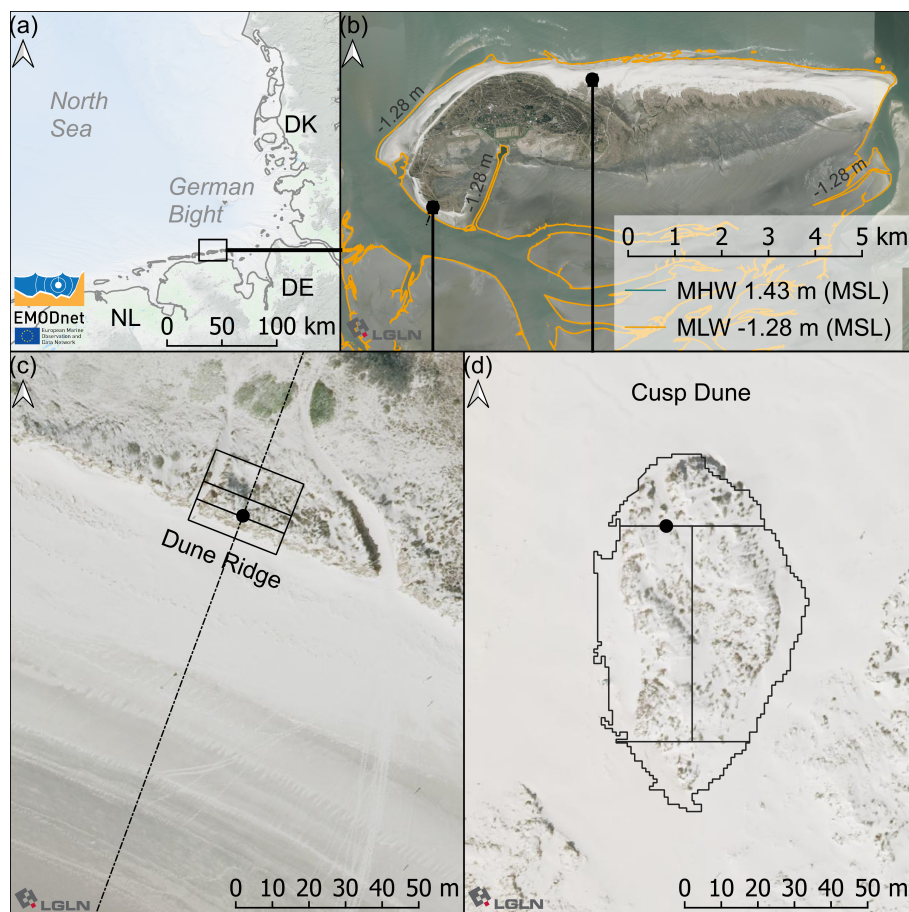


Figure 1. (a) Map of the German Bight with the focus area location. Based on EMODnet <https://emodnet.ec.europa.eu/en/bathymetry>. (b) Tidal barrier island Spiekeroog with tidal high and low water contour based on gauge data (GDWS, 2024) and DEM (NLWKN, 2023) and the two dune locations marked. (c) Dune ridge site and (d) cusp dune site - based on digital elevation model data (DEM) by Landesamt für Geoinformationen und Landesvermessung Niedersachsen (LGLN, engl.: State agency for geoinformation and state survey of Lower Saxony) data (LGLN, 2024). Mean high water (MHW) and mean low water (MLW) are extracted from the DEM using gauge related tidal water levels.

luv-side (sea-facing side, 160 m^2), dune crest (135 m^2), lee-side (land-facing side, 240 m^2). The Cusp Dune site (see Fig. 3) was segmented by geographical exposition into four zones: North (N, 550 m^2), East (E, 1490 m^2), West (W, 1497.5 m^2), and South (S, 350.5 m^2). The dune toe was extracted from DEM data using a 5° slope as delineation filter for both sites.

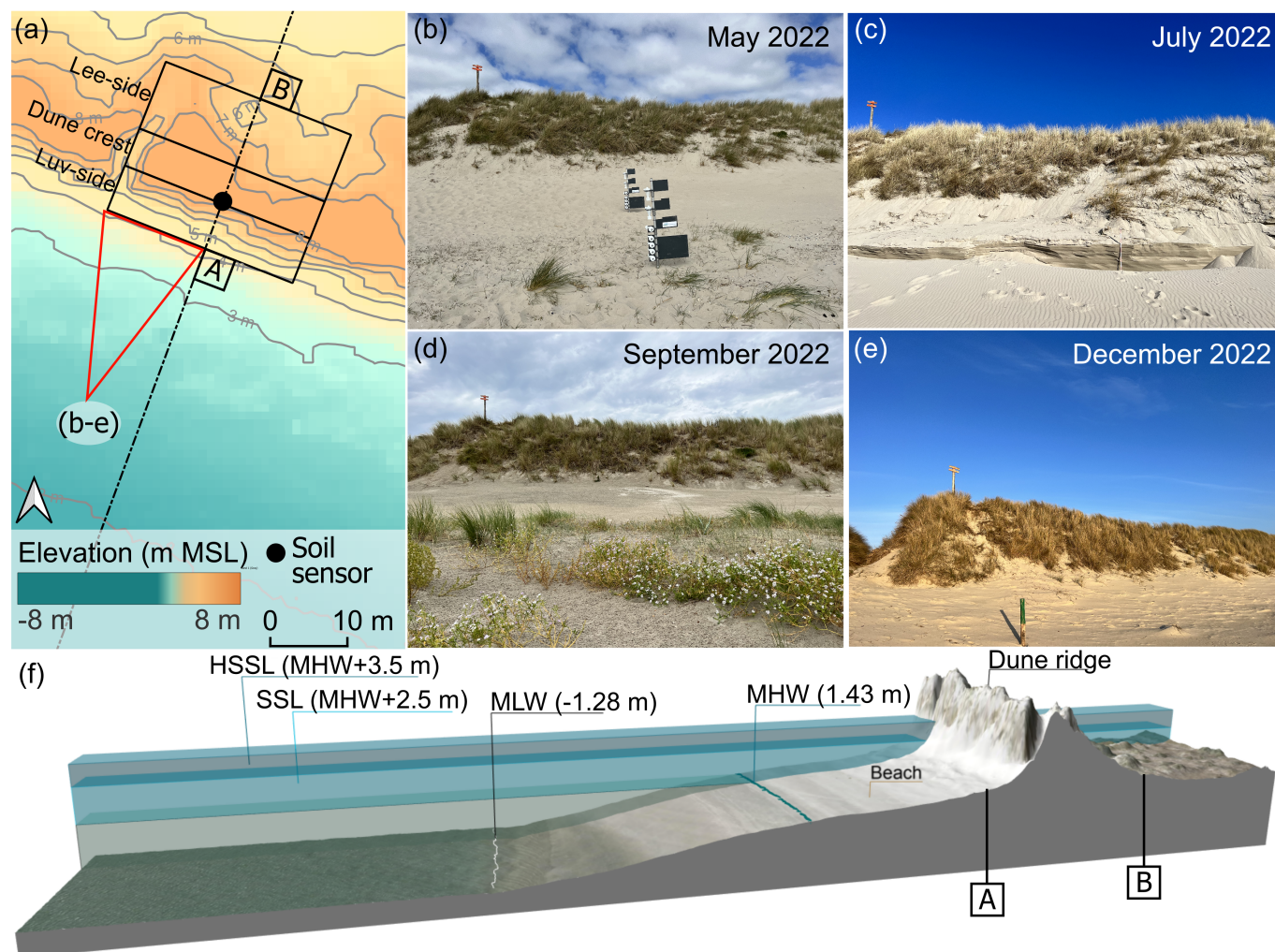


Figure 2. (a) Dune ridge sectors with elevation based on a 2022 DEM (NLWKN, 2023), and positioning of the soil sensor. (b-e) View of the luv-side of the dune during different seasons. (f) Cross shore profile based on 2022 DEM, vertically superelevated by a factor of 3. For details on soil sensor information see Appendix C.

195 2.2 Field data collection

Field data was acquired monthly from January 2022 to December 2022 at the two dune sites. The data collection focused on (1) environmental parameters, (2) canopy height and horizontal density, and (3) plant sampling for laboratory analysis.

Environmental parameters

200 Detailed measurements of environmental parameters, including soil temperatures via soil sensors at both dune sites (see Figures 2 and 3), air temperature and precipitation, as well as wind forces, were collected. These data, along with methodological

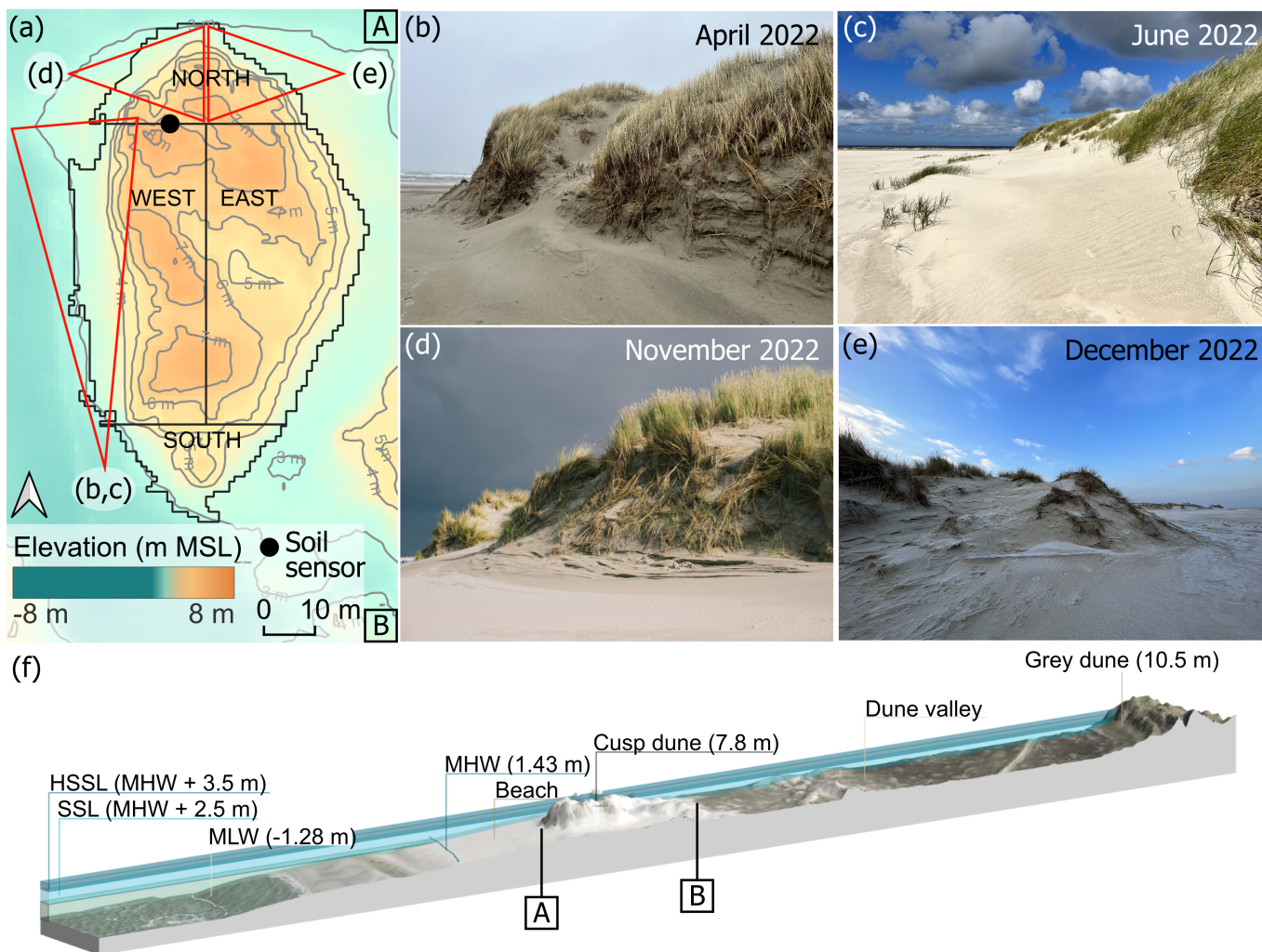


Figure 3. (a) Cusp dune outline and sectors with elevation based on a 2022 DEM (NLWKN, 2023), and positioning of the soil sensor. (b) View of the western slope of the dune in spring and (c) in summer. (d) View of the north-western edge in autumn and (e) view of the north-eastern edge in winter. View angles are indicated on (a) in red. (f) Cross shore profile based on 2022 DEM. For details on soil sensor information see Appendix C.

details and further findings, are provided in the Appendix (Sect. C).

Canopy height and horizontal density

205 Canopy height and horizontal density (see also Fig. A1a-b, Sect. A1 in the Appendix) were measured in different quantities depending on the zone and dune site. For the Dune Ridge site, which consists of three zones (luv-side, dune crest, and lee-side), 20 measurements were taken in both the luv-side and lee-side zones, and 10 measurements at the dune crest per month. For the



Cusp Dune site, which consists of four zones (North, East, South, West), 20 measurements were taken in both the North and South zones, and 30 measurements in the East and West zones per month. Height measurements, referred to as canopy height, were conducted with a ruler with an accuracy of 1 mm. Canopy height was determined as the mean of random measurements representing the lower and upper boundaries of the canopy. Horizontal density was assessed using a metal frame with an internal area of 20 cmx20 cm. The number of individual shoots within the frame was manually counted to determine the horizontal density. During the flowering season, the number of flowers was also counted within the same area but recorded separately. These values were later extrapolated to one square meter. Measurements were taken at random locations with vegetation cover to equally represent dense and sparse areas. All measurements were consistently conducted by the same individual to minimize observer bias.

Plant sampling

Plant sampling focused on the dominant species, marram grass. For the Dune Ridge site, 20 samples were taken from both the luv-side and lee-side zones, and 10 samples from the dune crest zone per month for further laboratory analysis (e.g., three-point bending tests). For the Cusp Dune site, 20 samples were collected from both the North and South zones, and 30 samples from the East and West zones per month. Individual shoots and, during the flowering season, an additional three flower stems (hereafter referred to as stems) per zone and month were cut at ground level using garden scissors. The cut was angled towards the west using a digital compass, leaving a point at the sample bottom pointing west. This method ensured that the orientation of the plant in the field could be tracked in the laboratory, maintaining consistent loading direction during biomechanical tests, which might be influenced by wind exposure (see also Sect. A1 in the Appendix).

2.3 Laboratory analysis

The laboratory analysis involved dividing the collected samples into their individual structural components and conducting three-point bending tests to assess their biomechanical properties

Sample preparation and plant parts

The sampled shoots of marram grass were divided into three main structural components: sprout, green leaf, and brown leaf. The sprout was defined as the lower part of the shoot up to the first branching leaf. In the laboratory, the sprout was separated from the shoot by cutting at this point. Leaves were also separated at their point of branching from the shoot. During the flowering season, stems, including the flower, were also collected and treated as a separate component, thus not requiring cutting (see also Sect. A1 in the Appendix).

For each zone and month, ten sprouts, three green leaves, three brown leaves, and, if applicable, three stems were analyzed. The samples were processed and tested within 1-2 days; prior to processing, they were stored upright in a vase-like container with a small amount of water to prevent wilting.



Measurement of length and outer diameter

The length (L) and outer diameter (d_o) of each plant part were important geometric parameters for biomechanical analysis. Lengths were measured in centimeters using a tape measure with an accuracy of 1 mm, though the practical reading accuracy
245 may be lower. The outer diameter was measured at the location where the three-point bending tests were to be conducted: at half the length ($L/2$) for sprouts and stems, and at one-third the length ($L/3$) for leaves (see also Sect. B1 in the Appendix). These diameters were measured using a digital caliper with a resolution of 0.01 mm.

Three-point bending tests

250 The three-point bending tests were performed according to ISO 178 (2019). Each plant part was cut into 6 cm long sections, with the measurement point of the outer diameter d_o located at the midpoint of these sections.

The bending tests utilized a universal testing machine, the „zwickiLine 500 N“ by ZwickRoell GmbH & Co.KG. This machine was equipped with a load cell, calibrated in compliance with DIN EN ISO 7500-1 (2018), ranging from 0.2 N to 50 N. The displacement measurement had an uncertainty of 0.0830 μm . The loading edges and supports had radii of 5 mm, and
255 the span between the supports (Δs) was 40 mm. The displacement rate was maintained at 0.05 mm/s, adhering to quasi-static deformation standards outlined by Liu et al. (2021). A preload of 0.05 N was applied to the samples before measurements commenced.

The bending tests produced force-deflection curves, which were essential for analyzing the mechanical properties of each sample. From these curves, the force (F) and deflection (D) were used to compute the bending stiffness ($K_B = F/D$, hereafter
260 referred to as stiffness) and the Young's modulus E of each sample, calculated from the initial slope of the force-deflection curve. In this study, the deflection range selected was between 0.4 mm and 1.2 mm, based on the initial linear portion of the force-deflection curve observed across all samples. Assuming an approximately circular solid cross-sections of the plant components, the Young's modulus was determined using the following equation:

$$E = \frac{4(\Delta s)^3 F}{3D\pi(d_o)^4} \quad (1)$$

265 The outer diameter (d_o) was used to simplify the calculation of the second moment of inertia (I), using the equation:

$$I = \frac{\pi(d_o)^4}{64} \quad (2)$$

The flexural stiffness (EI) was then calculated by multiplying Young's modulus (E) by the second moment of inertia (I).

The maximum force (F_{\max}), also referred to as the breaking force, was determined as the peak value on the force-deflection curves (Zhu et al., 2020; Liu et al., 2021). For marram grass, failure is more accurately characterized by folding rather than
270 breaking. The flexural strength σ was then calculated using the equation:

$$\sigma = \frac{40d_o F_{\max}}{8I} \quad (3)$$

The results from the bending tests provide a valuable data set (Kosmalla et al., 2024) of the plant components, such as Young's modulus (E), stiffness (K_B), flexural stiffness (EI), and flexural strength (σ). These parameters are vital for un-

derstanding the mechanical behavior of marram grass, which plays a crucial role in the resilience and adaptation of dune
275 ecosystems.

2.4 Data analysis

To streamline the data analysis process and enhance the interpretation of the results, the monthly data were aggregated into
seasonal intervals. The seasons were defined as "summer" (April to September) and "winter" (October to March). This catego-
rization reflects the primary dune dynamics: erosion processes, which predominantly occur in winter, and accretion processes,
280 which mainly happen in summer (Pye and Blott, 2016). This differentiation aims to capture potential seasonal variations in
the biomechanical properties of marram grass, relevant for experimental modeling of natural dune dynamics. An exception to
this seasonal aggregation was made for the analysis of wind influence and dune site comparisons, where year-round data were
considered.

For the analysis of biomechanical properties, the data from both dune sites were aggregated. This includes parameters such
285 as canopy height, horizontal density, number of flowers, and the biomechanically relevant properties of the individual plant
components (sprout, stem, green/brown leaf): Length, outer diameter, stiffness, and Young's modulus. Exceptions include the
investigation of wind influence, where data from the Dune Ridge were compared between the windward (luv) and leeward (lee)
sides. For the Cusp Dune, the zones were aggregated into Northwest (North and West) and Southeast (South and East). This
approach for the Dune Ridge is based on the assumption that the landward side is more sheltered from the wind, while for the
290 Cusp Dune, it is more directly based on the actual wind conditions during the study year. For the comparison between dune
sites, the data for each site were aggregated across all months and zones.

In total, 1543 sprout samples (Dune Ridge: 491, Cusp Dune: 1052), 389 stem samples (Dune Ridge: 115, Cusp Dune: 274),
831 green leaf samples (Dune Ridge: 227, Cusp Dune: 614), and 823 brown leaf samples (Dune Ridge: 224, Cusp Dune:
599) were investigated. The aggregated data were analyzed using Mann-Whitney U tests to statistically examine the following
295 comparisons:

1. Biomechanical differences between plant parts: The biomechanical parameters (K_B , E , d_o , L) of sprouts, green leaves,
brown leaves, and stems were compared seasonally to determine whether different plant parts exhibit distinct biome-
chanical properties. This analysis aggregated data from both dune sites.
2. Seasonal variations: The biomechanical parameters (K_B , E , d_o , L) of each plant part were compared between the "sum-
300 mer" (April to September, relevant for accretion processes) and "winter" seasons (October to March, relevant for erosion
processes) to detect any significant seasonal variations in the biomechanical properties of the dune vegetation. This
analysis aggregated data from both dune sites.
3. Impact of wind exposure and geographical exposition: The biomechanical parameters (K_B , E , d_o , L) of each plant part
were compared for the Dune Ridge site between windward (luv-side) and leeward (lee-side) zones, and for the Cusp Dune
305 site between Northwest and Southeast zones to evaluate the influence of wind exposure and geographical exposition on
biomechanical traits.



310

4. Differences between dune systems: The biomechanical parameters (K_B , E , d_o , L) of each plant part from the Dune Ridge (fixed, established dune system) and Cusp Dune (more dynamic dune system) sites were compared. For each plant component, data from the entire site, aggregated across all months and zones, were compared between the two dune systems to investigate how biomechanical properties differ between these two types of dune systems.

3 Results

3.1 Seasonal variations in biomechanical properties of marram grass

3.1.1 Geometric characteristics

Canopy height, horizontal density, and number of flowers

315

Canopy height (Fig. 4a) showed no significant difference between summer (79.66 ± 15.62 cm) and winter (79.87 ± 13.38 cm) measurements ($p = 0.3429$). Horizontal density (Fig. 4b), however, was significantly higher in summer (493.49 ± 217.97 shoots per m^2) compared to winter (445.65 ± 209.93 shoots per m^2 , $p < 0.001$). The number of flowers (Fig. 4c), observed only in summer, was on average 108.86 ± 92.50 flowers per m^2 . The results of the statistical analysis are provided in the Appendix (Sect. D, Table A1).

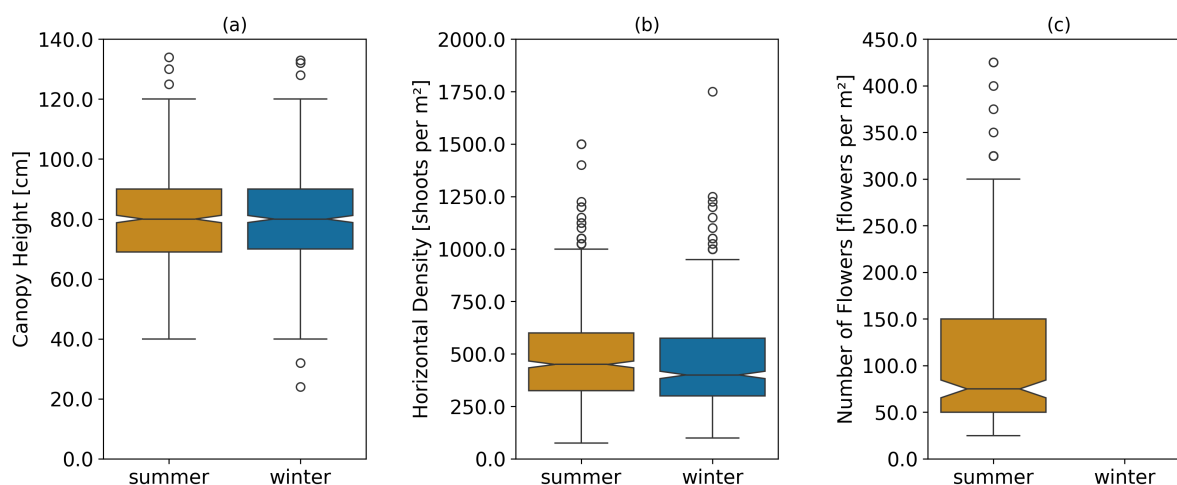


Figure 4. Combined data from both dune sites showing (a) Canopy height in cm, (b) Horizontal density in shoots per m^2 , and (c) Number of flowers in flowers per m^2 , comparing summer and winter illustrated as boxplots.

320

Length and outer diameter of plant components

The seasonal length and outer diameter of plant components are shown in Fig. 5a and b, respectively. Sprouts showed no significant seasonal variation in length between summer (18.28 ± 5.11 cm) and winter (15.37 ± 4.45 cm, $p = 0.196$). The outer diameter of sprouts also remained consistent across seasons (summer: 3.24 ± 0.53 mm, winter: 3.10 ± 0.51 mm, $p = 0.909$). Green

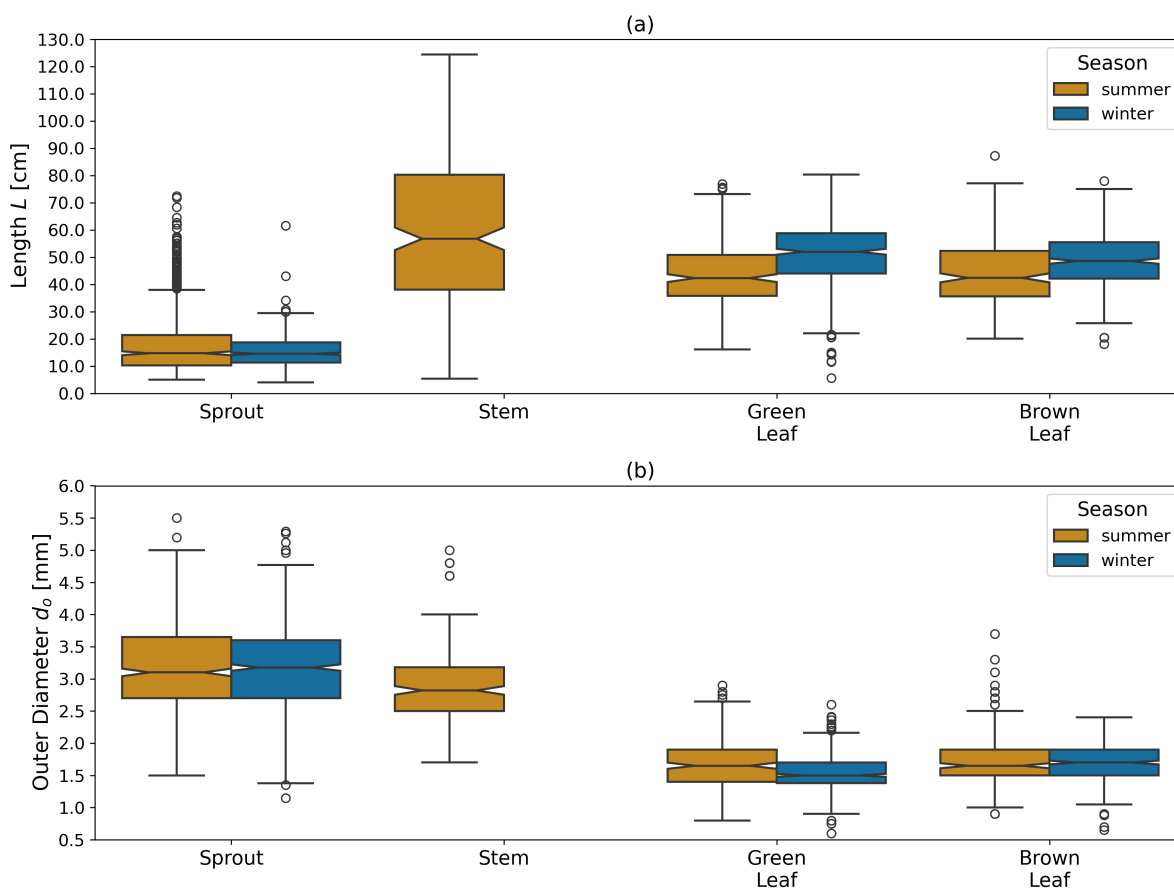


Figure 5. Combined data from both dune sites showing (a) mean length L and (b) mean outer diameter d_o of plant components (sprout, stem, green leaf, brown leaf) comparing summer and winter illustrated as boxplots.

leaves exhibited a significant increase in length during winter (51.47 ± 8.94 cm) compared to summer (44.35 ± 8.14 cm, $p <$
325 0.001). The outer diameter of green leaves was significantly larger in summer (1.69 ± 0.22 mm) than in winter (1.57 ± 0.20 mm, $p <$
0.001). For brown leaves, the length increased significantly from summer (43.80 ± 6.93 cm) to winter (47.82 ± 7.95 cm, $p <$
0.001). The outer diameter of brown leaves did not show significant seasonal variation between summer (1.72 ± 0.26 mm) and winter (1.67 ± 0.21 mm, $p = 0.199$) measurements. The length and outer diameter of stems were consistently measured in summer only, showing on average a length of 64.94 ± 10.87 cm and an outer diameter of 2.78 ± 0.39 mm. The results of the
330 statistical analysis are provided in the Appendix (Sect. D, Tables A2 and A3).

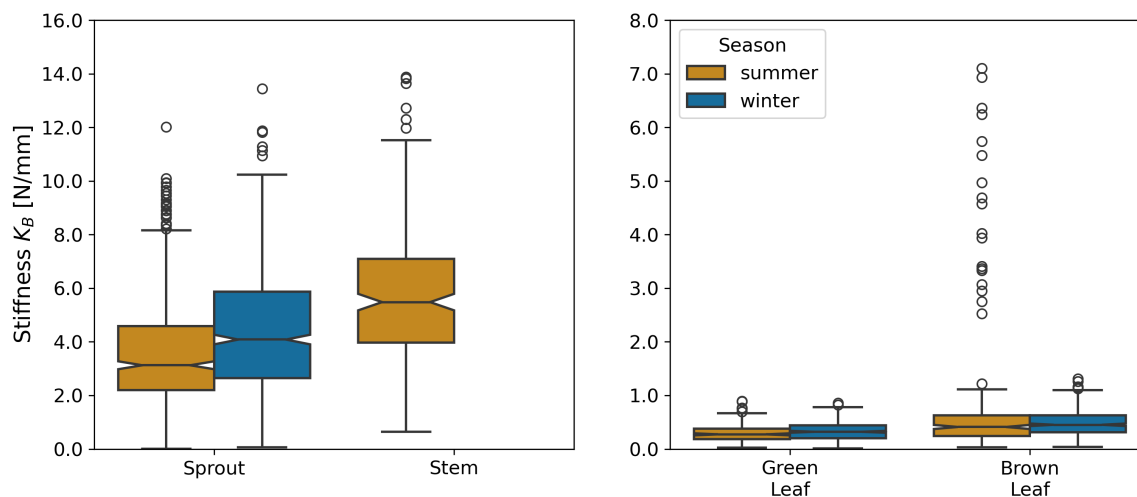


Figure 6. Stiffness K_B of each plant component in summer and winter months, based on combined data from both dune sites.

3.1.2 Mechanical characteristics

Stiffness

Stiffness showed significant seasonal variations in some plant components (see Fig. 6). For sprouts, stiffness was significantly higher in winter (4.15 ± 1.59 N/mm) compared to summer (3.98 ± 1.46 N/mm, $p < 0.001$). Green leaves also exhibited a significant seasonal difference, with higher stiffness in winter (0.33 ± 0.13 N/mm) than in summer (0.29 ± 0.11 N/mm, $p = 0.001$). Brown leaves showed no significant seasonal variation in stiffness (0.70 ± 0.46 N/mm in summer and 0.47 ± 0.18 N/mm in winter, $p = 0.077$). Stems were only measured in summer, with a mean stiffness of 5.30 ± 1.65 N/mm. The results of the statistical analysis are provided in the Appendix (Sect. D, Tables A2 and A3).

Young's modulus

Young's modulus displayed notable seasonal variations for certain plant components (see Fig. 7). For sprouts, Young's modulus was significantly higher in winter (1173.47 ± 479.92 MPa) compared to summer (1175.85 ± 563.72 MPa, $p < 0.001$). Green leaves also exhibited considerable seasonal differences, with Young's modulus being greater in winter (1585.21 ± 624.35 MPa) than in summer (1215.16 ± 526.92 MPa, $p < 0.001$). In contrast, brown leaves did not show significant seasonal variations in Young's modulus (1790.77 ± 809.09 MPa during summer and 1837.46 ± 855.73 MPa in winter, $p = 0.898$). Measurements for stems were only taken in summer, with a mean Young's modulus of 2641.05 ± 1152.78 MPa. The results of the statistical analysis are provided in the Appendix (Sect. D, Tables A2 and A3).

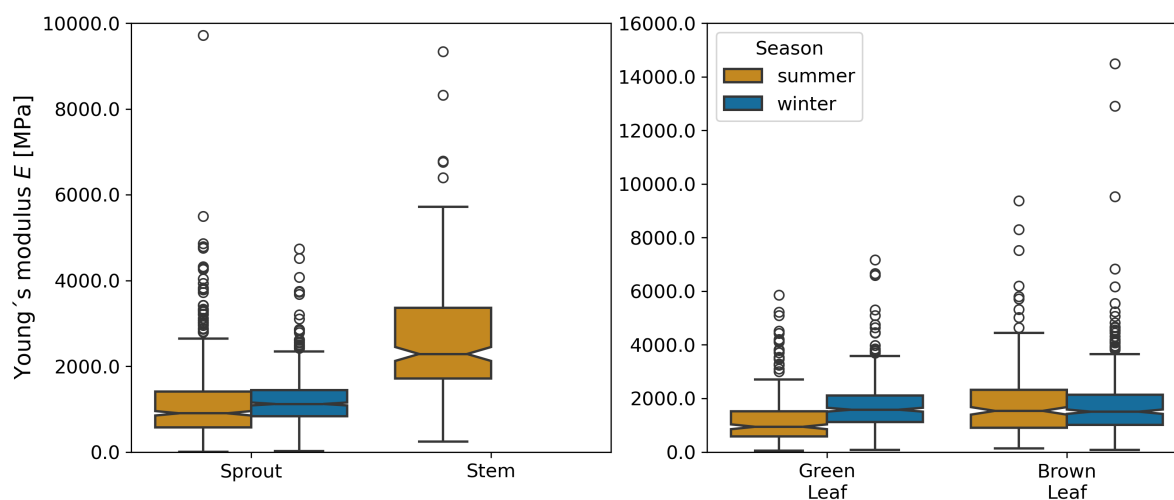


Figure 7. Young's modulus E of each plant component in summer and winter months, based on combined data from both dune sites.

3.2 Comparison of biomechanical traits among plant parts

Significant differences in the biomechanical parameters stiffness (K_B), Young's modulus (E), outer diameter (d_o), and length (L) were found between all plant components (sprouts, stems, green leaves, brown leaves) in both summer and winter (all $p < 0.001$), with the exception of Young's modulus between sprouts and green leaves in summer ($p = 0.319$), Young's modulus between green and brown leaves in winter ($p = 0.399$), and the outer diameter and length between green and brown leaves in summer ($p = 0.830$ and $p = 0.611$, respectively).

For stiffness (Fig. 6), all plant parts exhibited significant differences. In summer, stems had the highest stiffness values, followed by sprouts, brown leaves, and green leaves. During winter, the pattern remained consistent, excluding stems. In terms of the Young's modulus (Fig. 7), stems exhibited significantly higher values compared to other plant parts in summer. Brown leaves, green leaves, and sprouts followed. This order persisted in winter, excluding stems. Notably, there were no significant differences between sprouts and green leaves in summer, and between green and brown leaves in winter. For length (Fig. 5a), stems were significantly longer than the other parts in summer, with green leaves, brown leaves, and sprouts following. This trend remained in winter, excluding stems. In summer, no significant difference was found between green and brown leaves. Regarding outer diameter (Fig. 5b), sprouts had the significantly largest diameters in summer, followed by stems, brown leaves, and green leaves. In winter, the pattern remained consistent, excluding stems. The only exception was between green and brown leaves in winter, where the difference was not significant. The results of the statistical analysis are also provided in the Appendix (Sect. D, Table A4).



365 3.3 Impact of wind exposure on biomechanical traits

Stems exhibited no significant differences in any of the measured parameters (K_B , E , d_o , and L) between luv and lee-side or the Northwest and Southeast sides, respectively.

For Dune Ridge (see also Fig. 8, 10, and 12), the stiffness and Young's modulus of sprouts were significantly greater on the lee-side (4.40 ± 1.92 N/mm and 1374.14 ± 708.41 MPa) compared to the luv-side (3.31 ± 1.82 N/mm and 1048.84 ± 796.39 MPa, $p < 0.001$ for both parameters). Green leaves exhibited significantly greater stiffness (0.35 ± 0.17 N/mm), Young's modulus (1910.30 ± 1094.54 MPa), and length (52.44 ± 12.27 cm) on the lee-side compared to the luv-side (0.28 ± 0.15 N/mm, 1423.17 ± 842.79 MPa, and 44.92 ± 10.13 cm) with p -values of 0.010, 0.002, and < 0.001 respectively. Brown leaves showed no significant differences in stiffness, Young's modulus, and outer diameter between the luv and lee-side. However, the length of brown leaves was significantly greater on the lee-side (48.62 ± 11.87 cm) compared to the luv-side (43.28 ± 10.13 cm, $p = 0.003$).

Overall, all found trends at Dune Ridge indicate that the values of the respective parameters are significantly greater on the lee-side than on the luv-side.

For Cusp Dune (see also Fig. 9, 11, and 13), the Young's modulus (1162.39 ± 693.30 MPa) and length (17.20 ± 8.32 cm) of sprouts were significantly greater on the Northwest side compared to the Southeast side (1069.36 ± 637.48 MPa and 16.51 ± 9.51 cm with p -values of 0.020 and 0.015 respectively). Green leaves showed no significant differences in stiffness, Young's modulus, and length between the Northwest and Southeast sides. However, the outer diameter of green leaves was significantly greater on the Southeast side (1.63 ± 0.34 mm) compared to the Northwest side (1.57 ± 0.31 mm, $p = 0.030$). Brown leaves exhibited significantly greater stiffness (0.60 ± 0.81 N/mm) and Young's modulus (1686.62 ± 1041.84 MPa) on the Northwest side compared to the Southeast side (0.47 ± 0.51 N/mm and 1581.99 ± 1450.23 MPa, $p = 0.002$ and $p = 0.015$ respectively). While there is a tendency for the parameters stiffness, Young's modulus, and length to be greater in the Northwest, the outer diameter tends to be larger in the Southeast.

At both dune sites, the most significant differences were observed in the parameter Young's modulus, followed by stiffness and length, with the outer diameter showing the weakest differences.

390 3.4 Influence of dune systems on plant biomechanics

In comparing the biomechanical traits between the two dune systems, Dune Ridge and Cusp Dune, several significant differences were observed. Stems exhibited no significant differences in any of the measured parameters (K_B , E , d_o , and L) between Dune Ridge and Cusp Dune, indicating similar mechanical behavior across these systems for this plant part.

For sprouts, the Young's modulus was significantly higher at Dune Ridge (1243.01 ± 816.02 MPa) compared to Cusp Dune (1115.39 ± 666.96 MPa, $p = 0.002$). The outer diameter was significantly larger at Cusp Dune (3.20 ± 0.73 mm) compared to Dune Ridge (3.11 ± 0.63 mm, $p = 0.043$). Additionally, the length of sprouts was slightly greater at Dune Ridge (16.99 ± 11.23 cm) compared to Cusp Dune (16.85 ± 8.94 cm, $p = 0.039$).

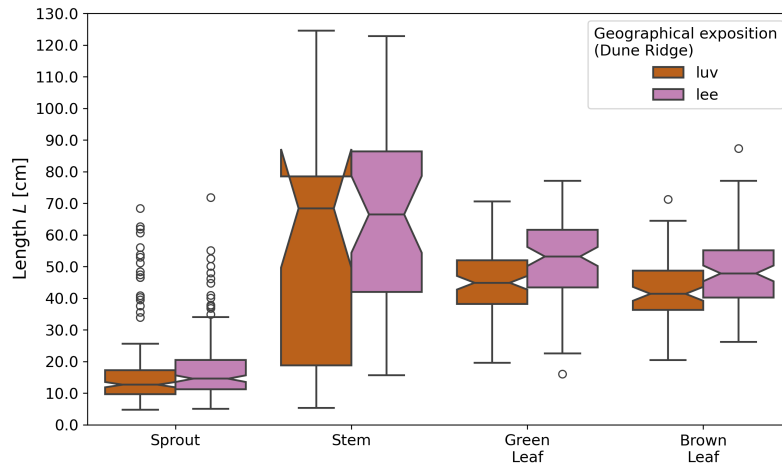


Figure 8. Comparison of luv-side and lee-side at Dune Ridge with boxplots showing length L for each plant component.

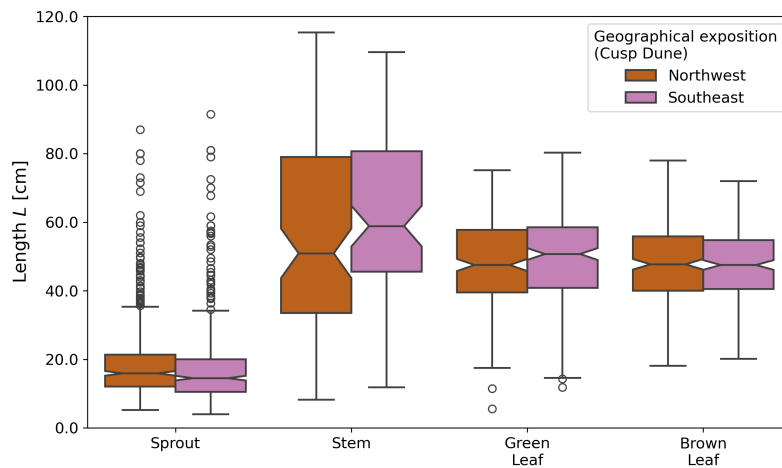


Figure 9. Comparison of "Northwest"-side and "Southeast"-side at Cusp Dune with boxplots showing length L for each plant component, based on year-round data.

Green leaves showed a significantly higher Young's modulus at Dune Ridge (1647.10 ± 1021.48 MPa) compared to Cusp Dune (1475.76 ± 972.71 MPa, $p = 0.031$). However, there were no significant differences in stiffness, outer diameter, and length.

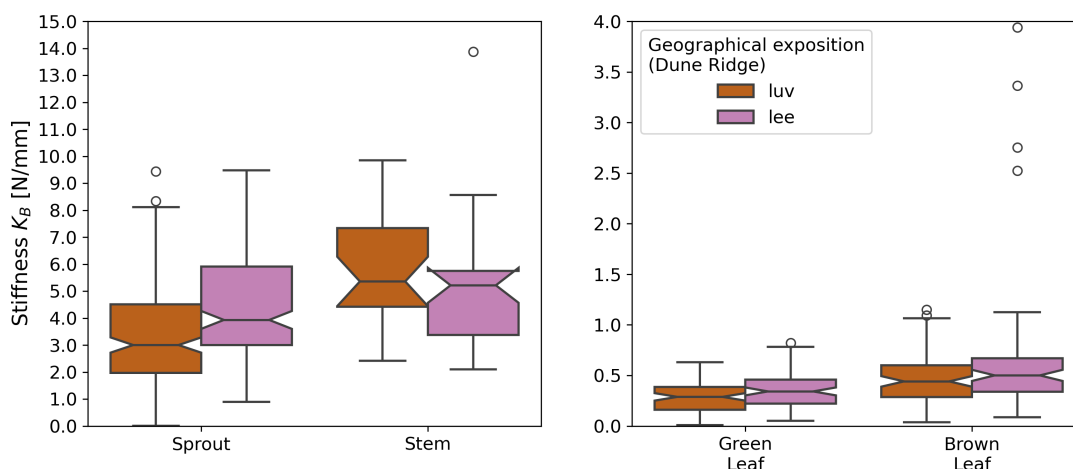


Figure 10. Comparison of luv-site and lee-site at Dune Ridge with boxplots showing stiffness K_B for each plant component, based on year-round data.

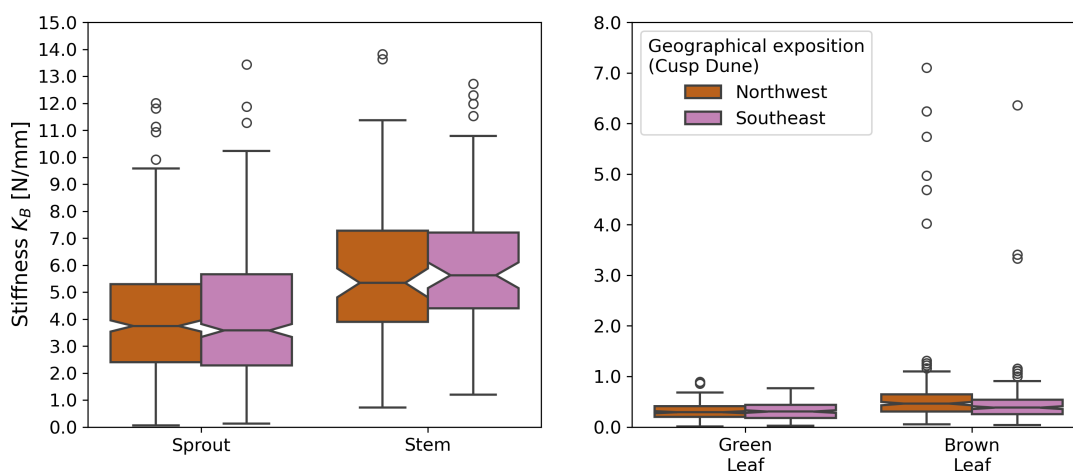


Figure 11. Comparison of "Northwest"-site and "Southeast"-site at Cusp Dune with boxplots showing stiffness K_B for each plant component, based on year-round data.

Brown leaves exhibited the most pronounced differences between the two dune systems. The Young's modulus was significantly higher at Dune Ridge (2159.01 ± 1425.67 MPa) compared to Cusp Dune (1634.93 ± 1260.05 MPa, $p < 0.001$), and the stiffness was also greater at Dune Ridge (0.63 ± 0.79 N/mm) compared to Cusp Dune (0.54 ± 0.68 N/mm, $p = 0.036$). The outer diameter of brown leaves was significantly larger at Cusp Dune (1.72 ± 0.30 mm) compared to Dune Ridge (1.65 ± 0.33 mm,

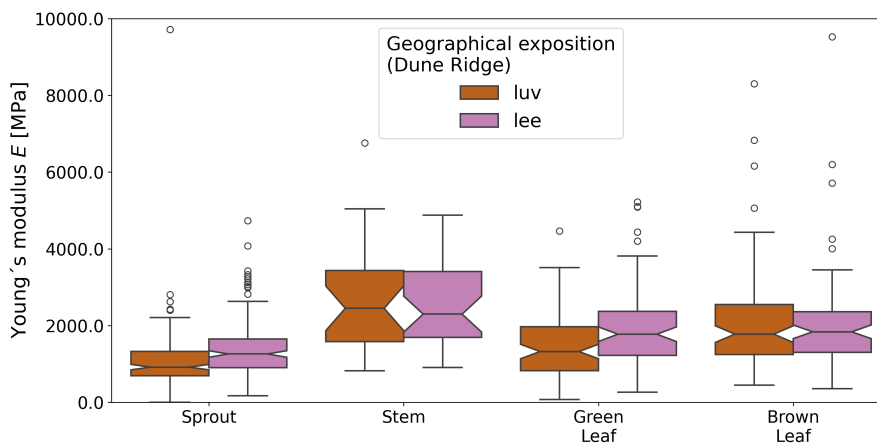


Figure 12. Comparison of luv-site and lee-site at Dune Ridge with boxplots showing Young's modulus E for each plant component, based on year-round data.

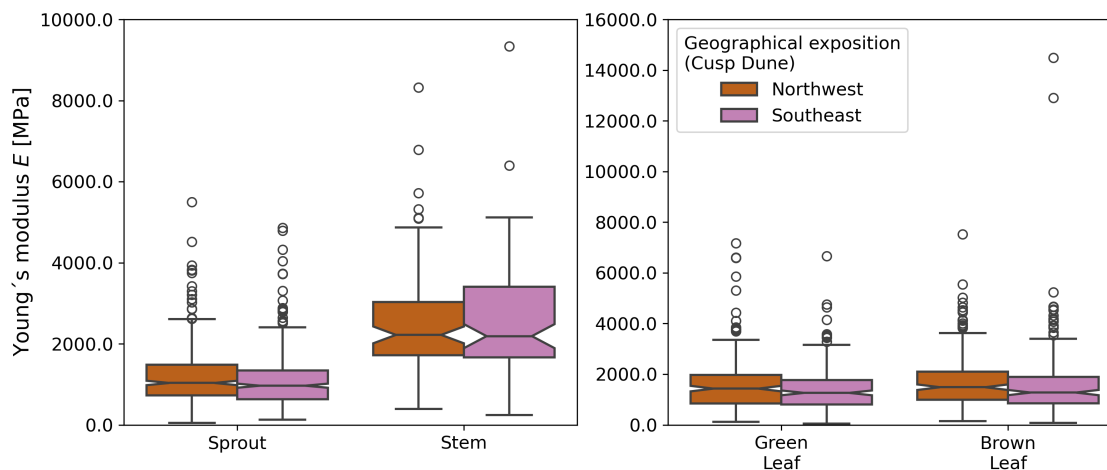


Figure 13. Comparison of "Northwest"-site and "Southeast"-site at Cusp Dune with boxplots showing Young's modulus E for each plant component, based on year-round data.

405 $p < 0.001$). The length of brown leaves was also significantly greater at Cusp Dune (47.35 ± 10.34 cm) compared to Dune Ridge (45.61 ± 11.34 cm, $p = 0.010$).

Overall, the Young's modulus was consistently higher at Dune Ridge across all plant parts except for stems. The outer diameter tended to be larger at Cusp Dune, particularly for sprouts and brown leaves. Length did not show a clear trend,

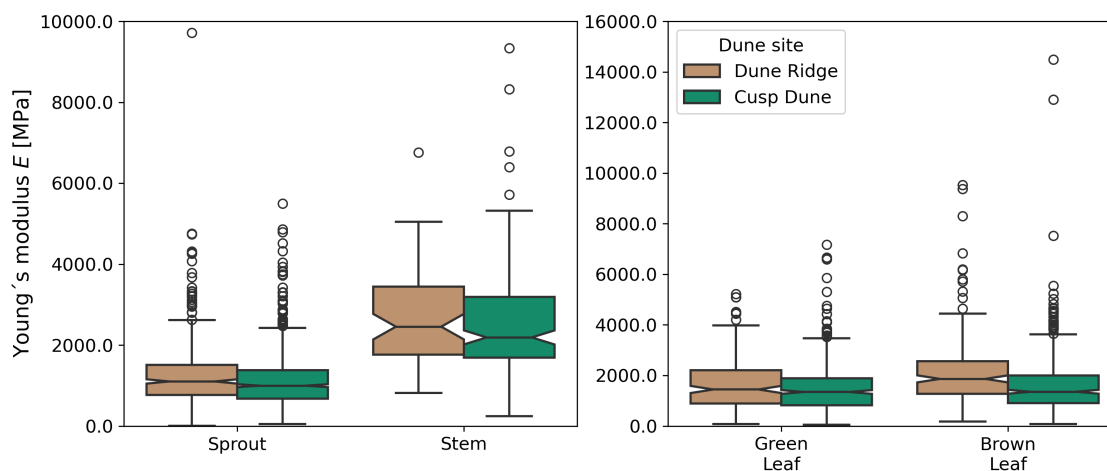


Figure 14. Comparison of dune sites (Dune Ridge and Cusp Dune) with boxplots showing Young's modulus E for each plant component, based on year-round data.

with significant differences observed only for sprouts and brown leaves. Stiffness differences were primarily notable in brown
410 leaves, with higher values at Dune Ridge.

4 Discussion

This study aims to provide detailed biomechanical parameters of marram grass to facilitate advanced modeling of dune vegetation. Current models often simplify or ignore traits in flexible vegetation, using surrogates like wooden dowels (e.g., Kobayashi et al. (2013); Bryant et al. (2019)), which do not accurately reflect the dynamic interactions between vegetation and dune environments. Our analysis incorporates the seasonality of dune dynamics, with accretion processes in summer and erosion processes in winter, as well as the growth cycles of the vegetation. This approach enables a more realistic simulation of the role of vegetation in dune stabilization and coastal defense strategies. In the following sections, we discuss our findings in detail, exploring the implications for improving the accuracy of dune vegetation models.

4.1 Seasonal variations in biomechanical traits

420 Understanding seasonal variations in plant properties is crucial for surrogate modeling because both dune dynamics and plant traits are subject to significant seasonal changes. Overall, our findings support the literature that during the summer, vegetation density significantly increases, while in the winter, the stiffness of the vegetation is greater and the outer diameter smaller (Koch et al., 2009; Vuik et al., 2017; Foster-Martinez et al., 2018; Keimer et al., 2024; Li et al., 2024). However, we observed that the length of vegetation, particularly green and brown leaves, tends to be greater in winter, contrasting those findings.



425 Overall, our findings confirm that while some parameters exhibit seasonal variability, others can be simplified for modeling purposes without losing accuracy.

For canopy height, no significant difference was observed between summer and winter, allowing the use of an annual average of 80 ± 15 cm, further specifying results by Hesp (1981) and Bressolier and Thomas (1977) who reported growth heights ranging from 50 to 100 cm.

430 Horizontal density was significantly higher in summer compared to winter, consistent with findings by Li et al. (2024) and Vuik et al. (2017), who noted increased vegetation density during the growth season. However, the density observed in this study was higher than the values reported by Seabloom and Wiedemann (1994) (203 stems m^{-2}) and Feagin et al. (2019) (260 stems m^{-2}), but fell within the range provided by Zarnetske et al. (2012) (up to $1000 \text{ tillers m}^{-2}$) and Hacker et al. (2012) ($480 \text{ plants m}^{-2}$). Our results showed that the number of flowers, observed only in summer, averaged $109 \pm 93 \text{ flowers m}^{-2}$,
435 which is significantly higher than the approximately $30 \text{ flowers m}^{-2}$ reported by Seabloom and Wiedemann (1994). This seasonal occurrence of flowers must be taken into account in modeling efforts.

For sprouts, significant seasonal variations were observed in both stiffness and Young's modulus, with higher values in winter compared to summer. The sprout length measurements can be compared to the stem heights up to 195 mm reported by Feagin et al. (2019), highlighting the importance of precise definitions of plant parts in such studies. Similarly, the sprout diameter
440 aligns with the stem diameter of 3 ± 1 mm found by Feagin et al. (2019). However, the differences identified in the findings are not substantial enough to significantly impact surrogate modeling, indicating that seasonal variations in these parameters are negligible for modeling purposes and thus can be averaged annually.

For stems, specifically flower stems, the summer-only presence highlights their importance for models representing the summer state. Their significant density, length, and high stiffness make them critical components in summer models where
445 their structural contribution to dune dynamics is essential. Since flower stems are only present in summer, these characteristics must be integrated into seasonal models but can be omitted in winter representations.

For green leaves, significant seasonal differences were observed in length, stiffness, and outer diameter. Besides stiffness, the length of green leaves was significantly greater in winter, which contrasts with the general trend observed in salt marsh vegetation, where lengths peak in summer (Li et al., 2024; Koch et al., 2009). This discrepancy may be due to the specific
450 growth patterns of marram grass, where older leaves persist through winter, contributing to greater overall lengths. Furthermore, this could also be attributed to the presence of younger, shorter plant parts during the growth phase in summer, which lowers the average length measurements. Conversely, the outer diameter of green leaves was larger in summer, which aligns with the findings of Vuik et al. (2017). However, the differences in stiffness and outer diameter between summer and winter were minor (summer: $0.29 \pm 0.11 \text{ kN/m}$ and $1.7 \pm 0.2 \text{ mm}$; winter: $0.33 \pm 0.13 \text{ kN/m}$ and $1.6 \pm 0.2 \text{ mm}$), making it practical to use
455 an annual average for these parameters in modeling efforts, especially for physical models where replicating such minor variations may be challenging.

For brown leaves, the only significant seasonal difference observed was in length, with brown leaves also being longer in winter. The stiffness and outer diameter of brown leaves did not exhibit significant seasonal variation, allowing these parameters to be averaged annually.



460 Overall, stiffness exhibited significant seasonal variations for both sprouts and green leaves, with higher values in winter compared to summer. This trend aligns with Vuik et al. (2017), who speculated that winter vegetation tends to be stiffer due to lower temperatures and the fracturing of less resilient parts. However, these differences are not substantial enough to significantly impact physical modeling, indicating that seasonal variations in these parameters are negligible for modeling purposes and thus can be averaged annually. However, the increased stiffness and Young's modulus in winter suggest that
465 dune vegetation is more resistant to mechanical stress during this period, potentially enhancing dune stability. Conversely, the greater flexibility and density in summer indicate a higher capacity for growth and dune accretion processes.

In summary, the significant seasonal variations in the biomechanical properties of marram grass highlight the need for seasonally adjusted modeling parameters in dune dynamics studies. Notably, three key aspects must be considered:

1. A major seasonal difference is the presence of flowers in summer, which must be accounted for in modeling.
- 470 2. The difference in horizontal density between seasons must be incorporated into surrogate models with an increased density in summer.
3. Besides flowers and density, only the length differences of the leaves are relevant and should be considered in modeling efforts.

4.2 Differentiation among plant parts

475 The variability in outer diameter and length among plant parts necessitates distinct consideration in modeling efforts. Sprouts and stems, with their larger diameters, offer robust resistance against physical forces. The differences in length, particularly the significant disparity between stems and other plant parts, further emphasize the need to account for each part's geometric characteristics to accurately represent their contributions to dune morphology. However, the lack of significant difference in outer diameter and length between green and brown leaves in summer, along with the relatively small differences in stiffness
480 and winter length, indicate that, for these parts, a simplified representation might be sufficient.

Given the close similarity between green and brown leaves, and considering the practicalities of physical modeling, where precise distinctions may not be easily implemented, the following simplified properties can be applied for leaves in general:

- Summer: Length = 44 ± 8 cm, Outer Diameter = 1.7 ± 0.2 mm, Stiffness = 0.45 ± 0.2 kN/m
- Winter: Length = 50 ± 9 cm, Outer Diameter = 1.7 ± 0.2 mm, Stiffness = 0.45 ± 0.2 kN/m

485 The significant differences in stiffness and Young's modulus between plant parts also underscore the need to model each component separately. Stems, with their highest values for both parameters, provide the greatest structural support. In contrast, green and brown leaves, which showed lower stiffness and Young's modulus, contribute more to flexibility and dynamic responses to environmental forces. These differences highlight the importance of including specific biomechanical properties for each plant part in models to accurately simulate their roles in dune stabilization and dynamics.

490 However, ignoring these differences could lead to inaccuracies in predicting vegetation behavior and its impact on dune dynamics, resulting in models that do not adequately reflect the true mechanical properties and structural roles of the vegetation.



It is crucial to distinguish between the biomechanical traits of each plant component to ensure the reliability of the models. The only exception to this are the green and brown leaves in summer, where the similarities suggest that a simplified approach may be appropriate without compromising model accuracy.

495 **4.3 Impact of wind on plant biomechanics**

The impact of wind exposure on the biomechanical traits of dune vegetation reveals significant variations between windward and leeward sides of the dunes, most notably in stiffness and Young's modulus. Stems exhibited no significant differences in any measured parameters between wind-exposed and sheltered sides, indicating uniform structural response. However, the greatest differences were observed in sprouts, with varying degrees of difference in green and brown leaves.

500 Significant differences in stiffness and Young's modulus between windward and leeward sides suggest these parameters are most sensitive to wind exposure. The higher values on the leeward side at Dune Ridge and in the northwest zone at Cusp Dune indicate different adaptive strategies. At Dune Ridge, the leeward side exhibited greater stiffness and Young's modulus, which may indicate an avoidance strategy, where vegetation minimizes the forces encountered by reducing exposure to wind through increased flexibility on the windward side. Conversely, at Cusp Dune, the northwest zone, which is more exposed to
505 wind, showed higher stiffness and Young's modulus, suggesting a tolerance strategy with vegetation maximizing its resistance to breakage to withstand wind forces.

Wind data from 2022 indicate that strong winds were predominantly west-dominated, with the highest frequency from the northwest during summer (see also Sect. C1 in the Appendix). As a result, the southwest-facing Dune Ridge coastline complicates wind exposure impact assessment. In general, comparisons between Northwest and Southeast zones showed few
510 significant differences, suggesting no strong wind exposure effect on plant biomechanics. Consequently, wind influence will not be included in the biomechanical parameterization of marram grass, serving as the basis for further surrogate modeling efforts.

4.4 Influence of dune type on plant biomechanics

The higher stem density and increased flower production in the Cusp Dune suggest favorable conditions for plant growth, such as frequent sand burial. This burial enhances the health and germination potential of the plants (Maun, 1998; Bonte et al., 2021;
515 van der Putten and Troelstra, 1990; Huiskes, 1979), leading to more frequent production of inflorescences compared to older, vegetative plants in fixed dunes. Higher canopy height in the North zone of the Cusp Dune suggests landward dune migration, emphasizing its categorization as a more mobile dune system. The presence of more flowers supports the view that the Cusp Dune is more dynamic, experiencing frequent morphological changes and higher sand deposition rates. In contrast, the Dune Ridge, as part of the fixed dunes, remains more stable (Isermann and Cordes, 1997; Pollmann et al., 2018).

520 The biomechanical properties of marram grass, particularly Young's modulus, exhibit higher stiffness on the fixed dune (Dune Ridge). However, this is not consistently confirmed by stiffness measurements, indicating no clear trend. The absence of a clear trend in these properties is beneficial for transferability, as it suggests that the same vegetation type (marram grass) exhibits robust biomechanical properties across different dune types. Stems show no significant trends, further supporting the idea of broad applicability of these findings. However, it is important to note that freshly planted marram grass for dune sta-



525 bilization or newly constructed dunes with planted vegetation might behave differently. This necessitates careful consideration
in modeling and practical applications.

4.5 Methodological considerations

4.5.1 Chosen plant species

The choice of marram grass for biomechanical parameterization was based on its widespread occurrence and historical use in
530 dune stabilization measures. Marram grass has been traditionally used in coastal management due to its strong root systems
and ability to trap sand, promoting dune formation and stability (Huiskes, 1979; Feagin et al., 2015; de Battisti and Griffin,
2020; Strypsteen et al., 2024), and thus was introduced for dune stabilization in different parts of the world (Bonte et al., 2021).
Additionally, the species' resilience to high temperatures and drought conditions, as demonstrated by temperature data (see
Sect. C3 in the Appendix), makes it an ideal candidate for future coastal defense strategies in the context of climate change
535 (Huiskes, 1979; Gao et al., 2020; Biel and Hacker, 2021).

4.5.2 Field investigations

Canopy height measurements were influenced by continuous morphological changes and seasonal accretion processes, pre-
dominantly occurring in summer, and erosion processes, predominantly occurring in winter. Evaluating canopy height in con-
junction with Digital Elevation Models (DEMs) provides a more comprehensive understanding of these dynamics and their
540 impact on dune morphology. However, such DEMs were not available for this study, highlighting the need for monthly surveys
and high-resolution aerial imagery to accurately capture these variations.

4.5.3 Laboratory investigations

Length and outer diameter measurements showed little annual variation, simplifying surrogate model creation. However, man-
ual diameter measurements using calipers are prone to inaccuracies due to non-circular cross-sections and potential sample
545 deformation. Additionally, the diameter of sprouts and stems can vary slightly along their length, and leaves naturally taper,
further complicating precise measurements. In studies of the biomechanical properties of salt marsh plants, such as those by
Rupprecht et al. (2015), Liu et al. (2021), Keimer et al. (2023) and Keimer et al. (2024), aboveground plant parts were di-
vided into three sections along their length to account for varying diameters. However, in this study, we maintain a simplified
approach for modeling, focusing on a more generalized representation of the plant structure.

550 Three-point bending tests maintained the natural orientation of the plants, minimizing the potential influence of varying wind
exposure. Previous studies by Keimer et al. (2023, 2024) on salt marsh species found no significant impact of orientation on
mechanical properties. However, practical challenges during testing, such as sample curvature and rolling, were noted. Leaves
exhibited variability in response due to their natural rolled structure, flattening under load. Additionally, the precision and
sensitivity of the force cell used in the bending tests, especially for leaves, presented a challenge due to the low stiffness.



555 Histological sections of marram grass' plant components (see also Sect. B1 in the Appendix) revealed the complex internal structure of the plants, highlighting their intricate cellular organization. This complexity, as previously shown by Andrade et al. (2021), poses significant challenges in precisely determining the second moment of inertia, a difficulty further demonstrated by Liu et al. (2021). For the biomechanical analysis, vegetation samples were assumed to have circular solid cross-sections. However, this assumption is a major limitation, as plant internal structures are often more complex. Leaves, for example, can
560 be open circles at certain points, raising concerns about the validity of the Young's modulus (E). This makes stiffness (K_B) a more reliable parameter, as it is less dependent on assumptions regarding cross-sectional geometry. Histological studies by Liu et al. (2021) on salt marsh plants indicated that the actual second moment of inertia could be 21 % lower than simplified calculations suggest. This underscores the necessity for detailed investigations into the internal structure of marram grass, particularly since sprouts possess an irregular structure with layers of leaf sheaths. Additionally, the cross-sectional area of
565 leaves varies depending on humidity and temperature, as demonstrated by Andrade et al. (2021), further complicating accurate biomechanical modeling.

4.6 Recommendations for future research

To build on the findings of this study and to further enhance our understanding of dune vegetation's biomechanical properties, particularly in the context of coastal protection, several key areas for future research are identified.

- 570 – Aboveground vegetation parts, which were the focus of this study's biomechanical parameterization, are crucial for processes such as dune growth and morphological development during the summer. Their sand-trapping properties are essential for dune formation and shaping (Feagin et al., 2015; Ruggiero et al., 2018), and the aboveground biomass creates drag, helping to prevent overwash and, as a result, preventing erosion on the landward side of the dune (Silva et al., 2016). However, belowground plant parts play a critical role in erosion processes and provide lateral resistance
575 of coastal dunes, particularly during extreme events (Feagin et al., 2019; Bryant et al., 2019; de Battisti and Griffin, 2020; Schweiger and Schuettrumpf, 2021; Figlus, 2022). Further data collection on belowground plant parts is needed to enhance our understanding of these processes and the potential impacts of abiotic stress, such as on root development (Gardiner et al., 2016; Kouhen et al., 2023). Implying belowground plant parts in future research was also stressed by Figlus et al. (2014), Silva et al. (2016), and Bryant et al. (2019). Husemann et al. (2024) and Freschet and Roumet
580 (2017) emphasize the importance of considering different parts of the below-ground biomass, such as roots, rhizomes, and buried shoots, each with distinct physical characteristics that contribute to the lateral resistance of coastal dunes, as was done here with aboveground plant parts.
- Experiments using real vegetation as well as surrogate models are necessary for comparison and validation, ideally on a large scale. This is particularly important given the challenges in accurately replicating the bending behavior of
585 vegetation. The use of 3D printing or other suitable materials, guided by the biomechanical properties of aboveground plant parts identified in this study, could enhance the accuracy of surrogate models. In this study, it is recommended to model each sprout with four leaves for more accurate representation, although this assumption has not been directly



validated within the scope of this research. Therefore, further verification is necessary to confirm this modeling approach and to ensure that it accurately reflects the natural vegetation structure. Additionally, the properties identified in this study must be seasonally distinguished in modeling efforts: summer values should be used for experiments focused on dune accretion processes, while winter values are more appropriate for modeling dune erosion processes. This seasonal differentiation is crucial for accurately simulating the dynamic interactions between vegetation and dune morphology throughout the year.

- Controlled studies on wind exposure effects and comparisons across different sites are recommended to better understand the influence of environmental factors on biomechanical properties. Expanding the dataset to include various locations and environmental conditions will enhance the reliability and applicability of surrogate models. Advanced techniques, such as machine learning, could be incorporated to predict vegetation behavior under diverse conditions. Additionally, a comprehensive comparison with newly constructed dunes planted with marram grass is important. Since marram grass planting is a common practice in coastal protection management (e.g., Gracia et al. (2018)), understanding its biomechanical properties in newly planted scenarios can provide valuable insights for effective dune stabilization strategies.
- While this study employed three-point bending tests due to their practicality and comparability with previous biomechanical studies of vegetation, future research might benefit from exploring two-point bending tests. Two-point bending tests could better simulate natural conditions, such as wind or wave-induced bending of above-ground plant parts. However, these tests are more demanding in terms of sample mounting and alignment, requiring more time and resources than were available in this study. The work of Liu et al. (2021), which employed such tests, underscores the need for appropriate sample fixation when considering this method.

5 Conclusions

This study provides a comprehensive dataset of the biomechanical properties of marram grass over 12 months, highlighting significant seasonal variations and differences among precisely defined plant components. By analyzing 841 green leaves, 823 brown leaves, 1543 sprouts, and 389 stems, we address the critical need for accurate representations of vegetation in the modeling of dune processes.

- **Seasonal variations:** The study identified significant seasonal variations in the biomechanical properties of marram grass. During winter, the vegetation exhibited increased stiffness and Young's modulus, indicating greater resistance to mechanical stress, which is crucial for erosion processes. In contrast, summer measurements showed greater flexibility and density, which are important for dune accretion. These findings suggest that modeling efforts should incorporate seasonally adjusted parameters to accurately represent the role of vegetation in different dune processes, particularly by accounting for differences in horizontal density, leaf length and the presence of flower stems in summer.
- **Differentiation among plant parts:** The biomechanical properties varied significantly between different plant parts, such as sprouts, green leaves, brown leaves, and flower stems. Stems provided the highest structural support due to their



620 greater stiffness and Young’s modulus, while leaves contributed more to flexibility and dynamic responses. The lack
 of significant differences between green and brown leaves, especially during summer suggests that these parts can be
 modeled similarly during, allowing for a simplified representation without losing accuracy.

– **Impact of wind forces:** The study found no consistent evidence that wind exposure significantly affects the biomechanical
 properties of marram grass. As such, wind influence will not be factored into the biomechanical modeling approach,
 625 though it remains a consideration for future research.

– **Dune type transferability:** The biomechanical properties of marram grass showed no clear trend between fixed and
 dynamic dune systems, supporting the transferability of the biomechanical data across different dune types. However, it
 is important to note that newly planted vegetation or newly constructed dunes might behave differently, indicating the
 need for careful consideration in such contexts.

630 In conclusion, this study addresses a significant gap in understanding the biomechanical properties of marram grass, provid-
 ing valuable insights for the development of accurate aboveground vegetation surrogates. The seasonal and plant-part specific
 traits identified in this research will enhance the reliability of models used to simulate dune dynamics and the role of vegetation
 in coastal defense. The following table (Table 1) provides a comprehensive overview of these properties, serving as a reference
 for future modeling efforts aimed at replicating the seasonal variations and structural characteristics essential for accurate dune
 635 process simulations.

Table 1. Summary of marram grass parameters for surrogate modeling to accurately represent seasonal variations in dune dynamics and
 vegetation.

General vegetation traits	Season	Value		
Canopy height (cm)	Annual	80 ± 15		
Horizontal density	Summer	494 ± 218		
(shoots m ⁻²)	Winter	446 ± 210		
Number of flowers	Summer	109 ± 93		
(flowers m ⁻²)	Winter	Not applicable		
Plant Part		Length (cm)	Outer diameter (mm)	Stiffness (N/mm)
Sprouts	Annual	17 ± 5	3.2 ± 0.5	4.1 ± 1.5
(Flower) Stems	Summer	65 ± 11	2.8 ± 0.4	5.3 ± 1.7
	Winter	Not applicable		
(Green and brown) Leaves	Summer	44 ± 8	1.7 ± 0.2	0.45 ± 0.2
	Winter	50 ± 9		

<https://doi.org/10.5194/egusphere-2024-2688>
Preprint. Discussion started: 25 September 2024
© Author(s) 2024. CC BY 4.0 License.



Data availability. The comprehensive data set presented in this study, detailing individual measurements from the monthly field campaign conducted from January to December 2022 on Spiekeroog, Germany, examining the geometrical and biomechanical properties of marram grass (*Calamagrostis arenaria*, formerly *Ammophila arenaria*), can be found in the following repository: <https://doi.org/10.24355/dbbs.084-202404230724-0>.



640 Appendix A: Plant sampling and methods

A1 Methods overview



Figure A1. Overview of the methodology used in this study. (a) Measurement of canopy height using a folding ruler. (b) Determination of horizontal density with a 20 cm frame. (c) Replacement of the data logger connected to the soil analysis sensor, with a close-up view in (d) showing the data logger within its enclosure during replacement. (e) Manufacturer's overview (Scantronik Mugrauer GmbH, 2024a) of the data logger (left) connected to the soil analysis sensor (right), which is installed approximately 20 – 30 cm deep in the soil. (f) Bundle of plant samples collected for further laboratory analysis. (g) Sample sections prepared for three-point bending tests. (h) Image of a sample in place for a three-point bending test before the start of the experiment.



A1 Plant sampling

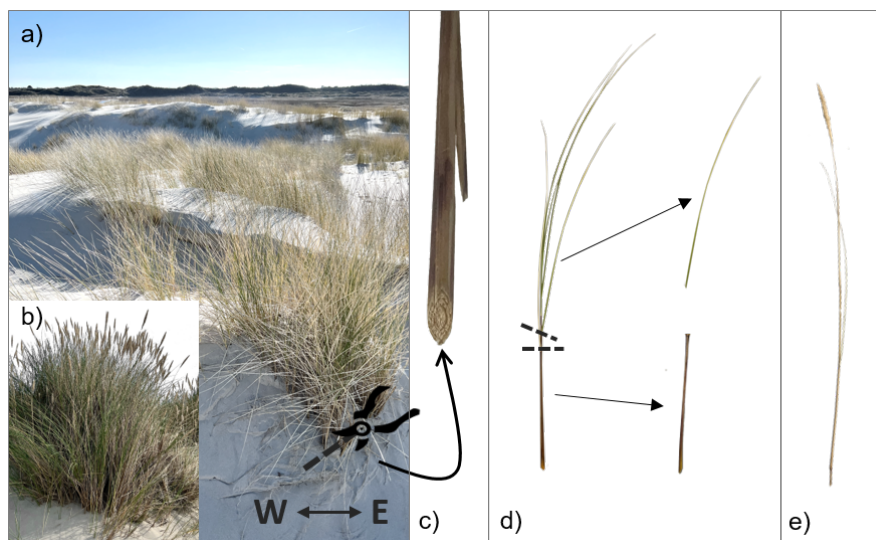


Figure B1. Overview of sample collection and preparation of marram grass. (a) Typical view of marram grass in winter (March 2022) with an illustration of the angled cutting technique used to ensure that the orientation of the samples in the field is maintained in the laboratory. Samples were cut and collected at the height of the soil surface. (b) Marram grass in summer (August 2022) showing high density and the presence of flowering stems. (c) Close-up of the cut end of a sample, indicating the longer side facing west. (d) A full shoot sample with cut sections for the removal of green/brown leaves (top) and sprouts (bottom), which are present year-round. (e) Separate image of a flowering stem after removal, relevant for the summer state of marram grass.



B1 Plant measurements



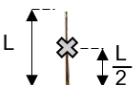
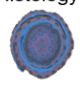
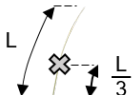
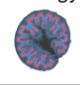
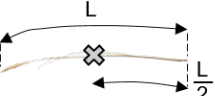
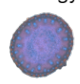
Plant part measurements		
 Length (L) of plant part  Measuring point for outer diameter (d_o) & bending test		
Sprout		
Sampling details: Bottom part of sample up to first leaf branching		Histology: 
Green / brown leaf		
Sampling details: Whole leaf from the point of leaf branching		Histology: 
Stem		
Sampling details: Cut only at ground level		Histology: 

Figure B2. Illustration of length (L) measurements, indicated by arrows, and measuring points marked with an "X" for defining the outer diameter (d_o) and the location of three-point bending tests. These measurements are demonstrated for the three plant component types: sprout, green/brown leaf, and (flowering) stem. Additionally, histological cross-sections are provided for each plant part to highlight the complexity of their internal structures.



Appendix C: Environmental parameters

645 Environmental parameters included soil temperature measurements taken at a depth of 20 – 30 cm using Soil Analysis Sensors
(Digital) by Scantronik Mugrauer GmbH. The measurement range for the temperature was -30°C to $+80^{\circ}\text{C}$, with an average
resolution of 0.1°C and an accuracy of $\pm 1^{\circ}\text{C}$. The positions of these sensors are marked in Figures 2a and 3a. Soil
temperature was recorded at 10-minute intervals with a Thermofox Universal data logger by Scantronik Mugrauer GmbH,
using Softfox (version 3.05) for setup. These recordings were first averaged over 60-minute periods to calculate hourly temper-
650 atures. For analysis purposes, the hourly temperatures were subsequently categorized into daytime and nighttime temperatures.
Daytime temperatures were defined as those recorded between 06:00 and 17:59, while nighttime temperatures were defined
as those recorded between 18:00 and 05:59. This separation of data allowed for a detailed examination of diurnal temperature
variations and their potential impact on dune vegetation. Due to a sensor failure at the Cusp Dune, there was a significant data
loss from May 2nd to July 13th, likely affecting the recorded temperatures in May, June, and July.

655 In addition to the soil sensor data, weather data were used to further describe the environmental conditions. The weather
data included wind measurements at 10 m height, air temperature, and precipitation for the years 2017-2022, with a particular
focus on wind data due to its presumed relevance to the biomechanical properties of the vegetation and its influence on ac-
cretion processes. Wind data were obtained from a weather station operated by the Deutscher Wetterdienst (DWD), located at
 53.7674°N , 7.6721°E on Spiekeroog. Air temperature and precipitation data were sourced from another weather station op-
660 erated by the Institute for Chemistry and Biology of the Marine Environment (ICBM) of the University of Oldenburg, located
nearby at 53.7762°N , 7.6880°E . Notably, all measurements were recorded at 10-minute intervals. Temperature and precipita-
tion data was subsequently averaged to monthly mean values.



C1 Wind forces

665 The wind roses (Fig. C1) illustrate the distribution of wind speed and direction for the years 2018-2022 (Fig. C1a) and the year
 2022 (Fig. C1b), along with seasonal data for 2022 (i.e., summer and winter, see Fig. C1c and d). During the years 2018-2022,
 strong winds (> 8 m/s, *Bft* 5) were west-dominated, totaling 64.46 % (W: 24.43 %, NW: 22.71 %, SW: 17.32 %).

In 2022, the distribution of strong winds shifted slightly, but remained west-dominated, totaling 66.61 % (W: 24.27 %, NW:
 26.59 %, SW: 15.75 %).

670 Focusing on summer months (April to September 2022), which represent key growth phases for vegetation, strong winds
 were predominantly from the northwest (W: 25.85 %, NW: 38.62 %). Moderate winds (< 8 m/s) were more evenly distributed,
 ranging from 8.52 % (SW) to 17.11 % (E).

In winter (October to March 2022), strong winds were more distributed and shifted slightly to the southwest (W: 22.97 %, SW:
 22.00 %, NW: 16.70 %). Moderate winds were predominantly from the south (S: 29.39 %, SE: 19.39 %, SW: 14.61 %).

675

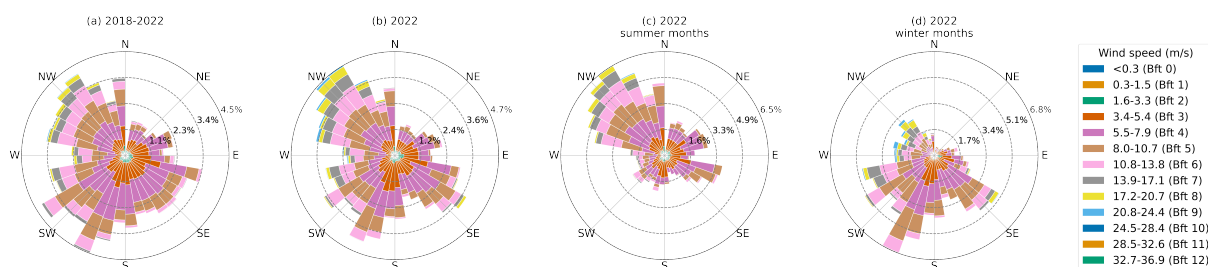


Figure C1. Wind roses showing wind direction and frequency for various time periods (Deutscher Wetterdienst): (a) wind rose for 2018-2022, (b) wind rose for 2022, (c) wind rose for summer months of 2022 (April-September), (d) wind rose for winter months of 2022 (October-March).



C2 Climate

The analysis of air temperature and precipitation data revealed that the air temperature peaks were consistently reached in July or August across all years, with August being the peak month in 2022 (Fig. C2). The lowest temperatures were observed from November to March in all years, with the winter of 2022 being relatively mild compared to other years, except for December. Overall, the air temperatures in 2022 were within the average range. Regarding precipitation, the data showed that 2022 had generally average precipitation levels with some outliers. Notably, February 2022 had a marked peak, recording the highest monthly average precipitation among all observed years.

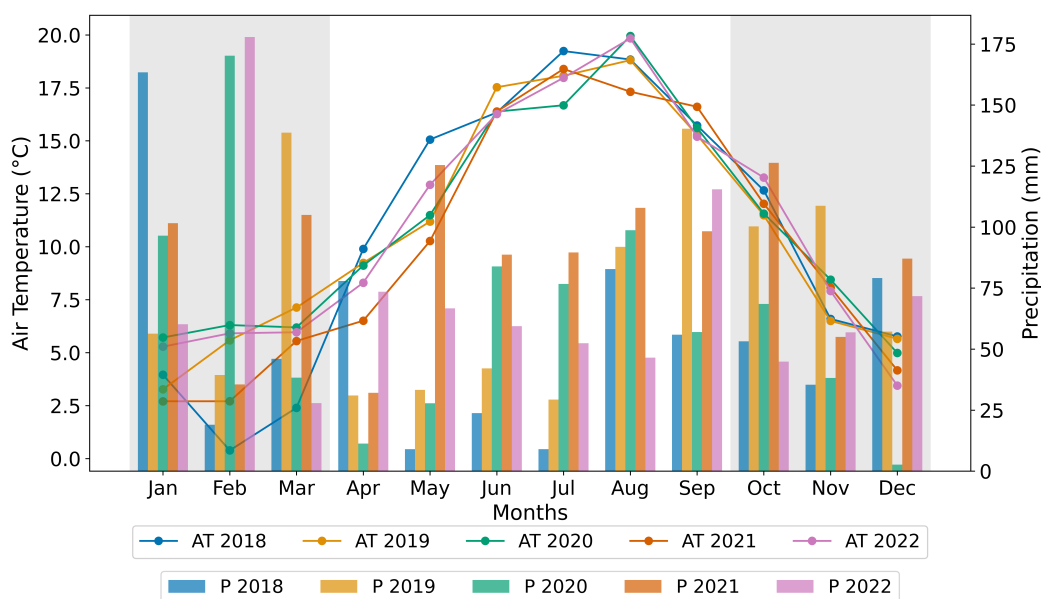


Figure C2. Markers and lines are showing monthly mean values of air temperature (in °C) and the bars monthly values of precipitation (in mm) for the years 2018-2022. White and gray background color indicate the definition of summer and winter months, respectively.

C3 Soil sensor

The soil temperatures at Dune Ridge and Cusp Dune sites showed considerable seasonal and diurnal variations throughout the 685 year 2022, as illustrated by the boxplots in Fig. C3.

Comparing the two sites, Dune Ridge (Fig. C3a) generally exhibited higher temperature extremes, especially during the day, reflecting potentially greater solar exposure due to sparse vegetation. For instance, in August, the maximum daytime soil temperature at Dune Ridge was 48.03 °C with an average of 28.02 °C, while at Cusp Dune (Fig. C3b), the maximum was 31.60 °C with an average of 23.30 °C. The highest daytime soil temperature recorded was 53.38 °C at Dune Ridge in July. 690 The surrounding vegetation at Cusp Dune, which grew tall and dense by June (Fig. C4-2a and -2b), likely shaded the sensor, contributing to lower recorded temperatures compared to Dune Ridge (Fig. C4-1a and -b).

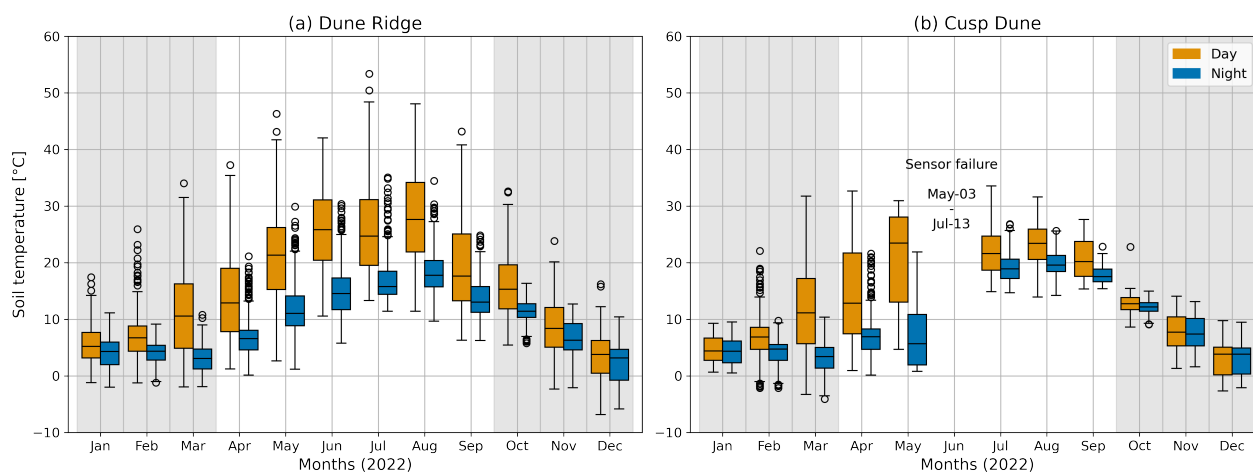


Figure C3. Monthly daytime (in orange) and nighttime soil temperatures (in blue) at (a) Dune Ridge and (b) Cusp Dune throughout 2022. White and gray background color indicate the definition of summer and winter months, respectively.



Figure C4. (1) Soil sensor at Dune Ridge (1a) in February 2022 and (1b) in November 2022. (2) Soil sensor at Cusp Dune (2a) in February 2022 and (2b) in June 2022. The images illustrate the differences in vegetation cover and shading at the sensor locations across different times of the year.

Appendix D: Biomechanical properties

This section presents a detailed exploration of the seasonal variations in the biomechanical properties of aboveground vegetation parts of marram grass. The analysis begins with heatmaps that illustrate how these properties change across different zones and seasons (see Fig. D1-D4). Following this visual representation, several tables (see Tables A1-A7) summarize the results of the statistical analyses, each addressing the key research questions of this study and providing a comprehensive overview of the significant findings related to the biomechanical traits of the vegetation.

D1 Seasonal variations in biomechanical properties of marram grass

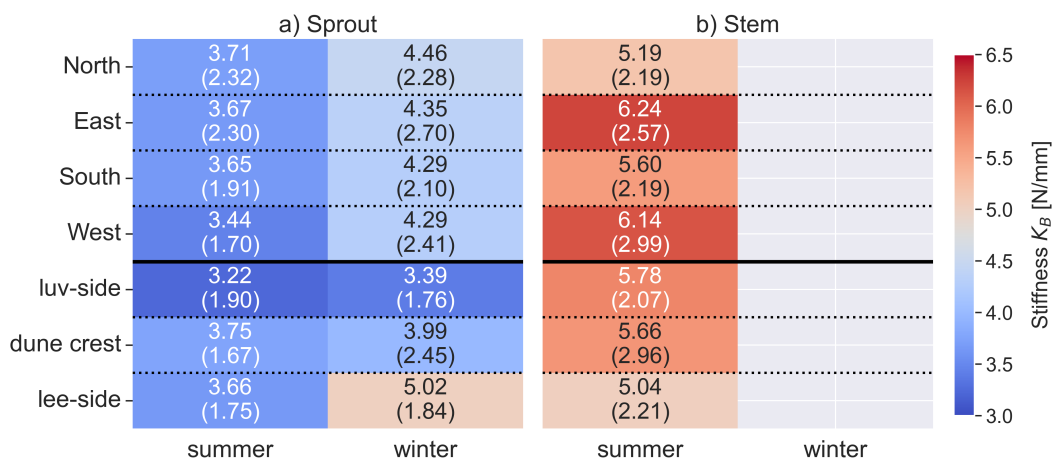


Figure D1. Heatmap showing stiffness K_B for (a) sprout and (b) stem in different zones and seasons. The values within the heatmap cells represent the mean stiffness (in N/mm) with the standard deviation in parentheses.

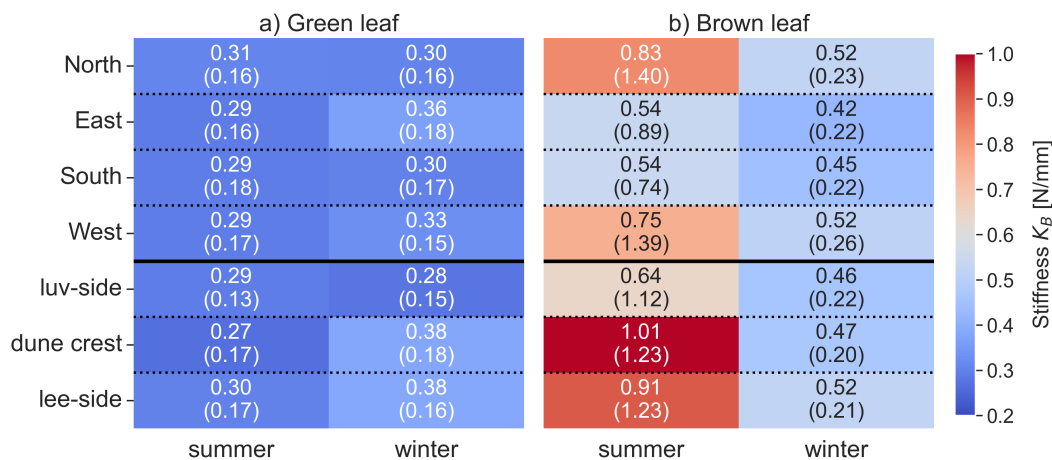


Figure D2. Heatmap showing stiffness K_B for (a) green leaf and (b) brown leaf in different zones and seasons. The values within the heatmap cells represent the mean stiffness (in N/mm) with the standard deviation in parentheses.

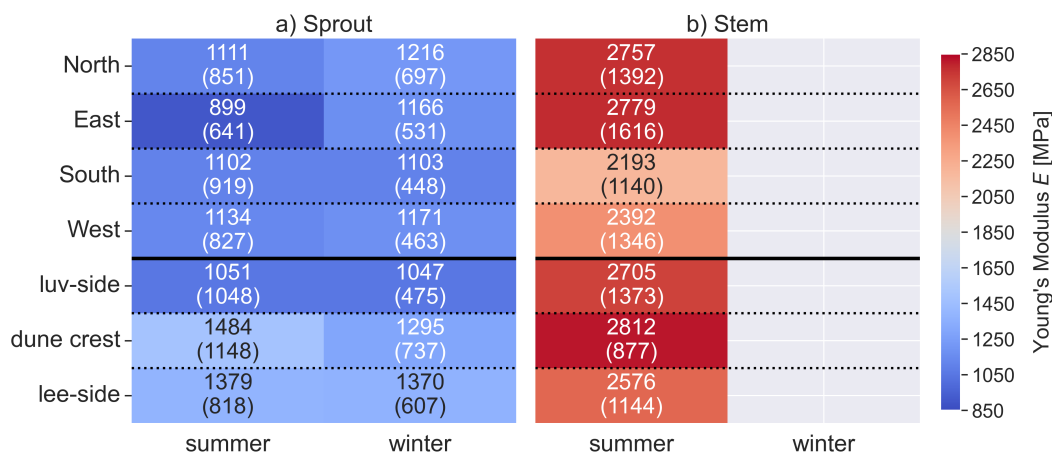


Figure D3. Heatmap showing Young's modulus E for (a) sprout and (b) stem in different zones and seasons. The values within the heatmap cells represent the mean Young's modulus (in MPa) with the standard deviation in parentheses.

700 **A1 Comparison of biomechanical traits among plant parts**

A2 Impact of wind exposure on biomechanical traits

A3 Influence of dune systems on plant biomechanics

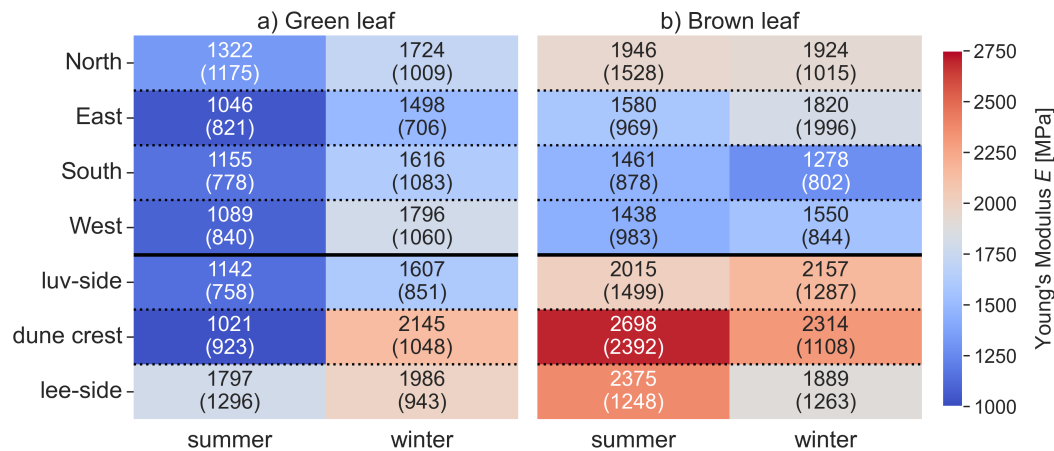


Figure D4. Heatmap showing Young's modulus E for (a) green leaf and (b) brown leaf in different zones and seasons. The values within the heatmap cells represent the mean Young's modulus (in MPa) with the standard deviation in parentheses.

Table A1. Mean and standard deviation of canopy height, horizontal density, and number of flowers for both dune sites across seasons (summer/winter) as well as Mann-Whitney U test results showing seasonal differences with significant values ($p < 0.05$) in bold.

Parameter	Unit	Season	mean	std	P-value
Canopy Height	[cm]	summer	79.66	15.62	0.343
		winter	79.87	13.38	
Horizontal Density	[shoots m^{-2}]	summer	493.49	217.97	<0.001
		winter	445.65	209.93	
Number of Flowers	[flowers m^{-2}]	summer	108.86	92.50	NaN
		winter	NaN	NaN	



Table A2. Mean and standard deviation of parameters for different plant components and dune sites across seasons (summer/winter).

			Stiffness K_B		Young's modulus E		Outer diameter d_o		Length L	
			[N/mm]		[MPa]		[mm]		[cm]	
Plant part	Dune site	Season	mean	std	mean	std	mean	std	mean	std
Sprout	Combined	summer	3.98	1.46	1175.85	563.72	3.24	0.53	18.28	5.11
	Combined	winter	4.15	1.59	1173.47	479.92	3.10	0.51	15.37	4.45
	Dune Ridge	summer	3.83	1.46	1252.04	649.42	3.14	0.51	19.04	5.11
	Dune Ridge	winter	4.19	1.53	1209.69	453.96	3.15	0.48	14.86	3.92
	Cusp Dune	summer	4.06	1.46	1134.94	518.45	3.29	0.54	17.90	5.12
	Cusp Dune	winter	4.14	1.62	1155.97	492.47	3.07	0.52	15.62	4.70
Stem	Combined	summer	5.30	1.65	2641.05	1152.78	2.78	0.39	64.94	10.87
	Dune Ridge	summer	5.13	1.48	2776.14	1002.39	2.69	0.32	65.42	9.47
	Cusp Dune	summer	5.39	1.74	2573.51	1230.58	2.83	0.43	64.70	11.57
Green Leaf	Combined	summer	0.29	0.11	1215.16	526.92	1.69	0.22	44.35	8.14
	Combined	winter	0.33	0.13	1585.21	624.35	1.57	0.20	51.47	8.94
	Dune Ridge	summer	0.29	0.11	1379.62	609.47	1.63	0.23	43.14	9.02
	Dune Ridge	winter	0.32	0.13	1755.47	626.07	1.52	0.21	50.84	8.12
	Cusp Dune	summer	0.29	0.11	1132.93	485.64	1.72	0.22	44.95	7.70
	Cusp Dune	winter	0.33	0.12	1502.92	623.52	1.59	0.20	51.77	9.33
Brown Leaf	Combined	summer	0.70	0.46	1790.77	809.09	1.72	0.26	43.80	6.93
	Combined	winter	0.47	0.18	1837.46	855.73	1.67	0.21	47.82	7.95
	Dune Ridge	summer	0.81	0.55	2248.17	1100.85	1.69	0.28	43.80	8.04
	Dune Ridge	winter	0.48	0.18	2159.45	943.93	1.61	0.24	46.43	8.62
	Cusp Dune	summer	0.64	0.41	1550.03	655.26	1.73	0.24	43.80	6.38
	Cusp Dune	winter	0.46	0.18	1681.84	813.11	1.70	0.20	48.47	7.64



Table A3. Mann-Whitney U Test results comparing seasonal differences (summer/winter) for each plant component, with data aggregated across both dune sites (Dune Ridge and Cusp Dune). Significant values ($p < 0.05$) in bold.

Part	Parameter	P-Value
Sprout	Stiffness K_B	<0.001
	Young's modulus E	<0.001
	Outer diameter d_o	0.909
	Length L	0.196
Green Leaf	Stiffness K_B	0.001
	Young's modulus E	<0.001
	Outer diameter d_o	<0.001
	Length L	<0.001
Brown Leaf	Stiffness K_B	0.077
	Young's modulus E	0.898
	Outer diameter d_o	0.199
	Length L	<0.001



Table A4. Results of the Mann-Whitney U tests comparing biomechanical parameters between plant components for each season. Significant values ($p < 0.05$) in bold.

Part A	Part B	Season	Parameter	P-Value	Part A	Part B	Season	Parameter	P-Value
Sprout	Stem	summer	K_B	<0.001	Green Leaf	Brown Leaf	summer	K_B	<0.001
			E	<0.001				E	<0.001
			d_o	<0.001				d_o	0.830
			L	<0.001				L	0.611
Sprout	Green Leaf	summer	K_B	<0.001	Green Leaf	Brown Leaf	winter	K_B	<0.001
			E	0.319				E	0.399
			d_o	<0.001				d_o	<0.001
			L	<0.001				L	<0.001
Sprout	Green Leaf	winter	K_B	<0.001	Green Leaf	Stem	summer	K_B	<0.001
			E	<0.001				E	<0.001
			d_o	<0.001				d_o	<0.001
			L	<0.001				L	<0.001
Sprout	Brown Leaf	summer	K_B	<0.001	Brown Leaf	Stem	summer	K_B	<0.001
			E	<0.001				E	<0.001
			d_o	<0.001				d_o	<0.001
			L	<0.001				L	<0.001
Sprout	Brown Leaf	winter	K_B	<0.001	Brown Leaf	Stem	summer	K_B	<0.001
			E	<0.001				E	<0.001
			d_o	<0.001				d_o	<0.001
			L	<0.001				L	<0.001



Table A5. Mann-Whitney U Test results comparing luv and lee (Dune Ridge) for each plant component. Significant values ($p < 0.05$) in bold.

Part	Parameter	P-Value
Sprout	Stiffness K_B	<0.001
	Young's modulus E	<0.001
	Outer diameter d_o	0.957
	Length L	0.168
Stem	Stiffness K_B	0.086
	Young's modulus E	0.642
	Outer diameter d_o	0.668
	Length L	0.159
Green Leaf	Stiffness K_B	0.010
	Young's modulus E	0.002
	Outer diameter d_o	0.622
	Length L [cm]	<0.001
Brown Leaf	Stiffness K_B	0.125
	Young's modulus E	0.689
	Outer diameter d_o	0.183
	Length L	0.003



Table A6. Mann-Whitney U Test results comparing Northwest and Southeast (Cusp Dune) for each plant component. Significant values ($p < 0.05$) in bold.

Part	Parameter	P-Value
Sprout	Stiffness K_B [N/mm]	0.748
	Young's modulus E [MPa]	0.020
	Outer diameter d_o [mm]	0.316
	Length L [cm]	0.015
Stem	Stiffness K_B [N/mm]	0.597
	Young's modulus E [MPa]	0.744
	Outer diameter d_o [mm]	0.526
	Length L [cm]	0.260
Green Leaf	Stiffness K_B [N/mm]	0.506
	Young's modulus E [MPa]	0.055
	Outer diameter d_o [mm]	0.030
	Length L [cm]	0.165
Brown Leaf	Stiffness K_B [N/mm]	0.002
	Young's modulus E [MPa]	0.015
	Outer diameter d_o [mm]	0.960
	Length L [cm]	0.568



Table A7. Mann-Whitney U Test results comparing Dune Ridge vs Cusp Dune for each plant component. Significant values ($p < 0.05$) in **bold**.

Part	Parameter	P-Value
Sprout	Stiffness K_B	0.347
	Young's modulus E	0.002
	Outer diameter d_o	0.044
	Length L	0.039
Stem	Stiffness K_B	0.439
	Young's modulus E	0.185
	Outer diameter d_o	0.061
	Length L	0.805
Green Leaf	Stiffness K_B	0.872
	Young's modulus E	0.031
	Outer diameter d_o	0.063
	Length L	0.277
Brown Leaf	Stiffness K_B	0.036
	Young's modulus E	<0.001
	Outer diameter d_o	<0.001
	Length L	0.010



Author contributions. VK, OL, and KK planned the campaign; VK, OL, and LA performed the measurements; VK, JC, and BS analyzed the data; VK wrote the manuscript draft; VK and OL prepared visualizations; OL, JC, KK, LA, BM, DS, BS, and NG reviewed and edited the manuscript; OL, DS, and NG administered the project and organized funding acquisition.

Competing interests. The authors declare that they have no conflict of interest.

Acknowledgements. This study was performed as part of the joint research project “Gute Küste Niedersachsen” funded by the Lower-Saxony Ministry of Research and Culture (FKZ: 76251-17-5/19) and the Volkswagen Stiftung. We are greatly indebted to the National Park Authority (Nationalparkverwaltung Niedersächsisches Wattenmeer) for providing site access and permission to use it for scientific research. We would also like to thank Mr. Malte Kumlehn and Mr. Leon Vinkelau, for assisting with field campaigns as well as supporting in the laboratory. The authors wish to thank Dipl. Phys. Frank Hillmann from the ICBM, University of Oldenburg, for providing weather data from Spiekeroog. Appreciation is also extended to Prof. Robert Hänsch from the Institute of Plant Biology at TU Braunschweig for valuable discussions about plant morphology. Special thanks go to Holger Dirks from the Coastal Research station of the Niedersächsischer Landesbetrieb für Wasserwirtschaft, Küsten- und Naturschutz (NLWKN) for providing high resolution digital elevation model data of Spiekeroog.



715 References

- Andrade, T., Beirão, J., Arruda, A., and Cruz, C.: The adaptive power of *Ammophila arenaria*: biomimetic study, systematic observation, parametric design and experimental tests with bimetal, *Polymers*, 13, <https://doi.org/10.3390/polym13152554>, 2021.
- Baas, A. and Nield, J. M.: Ecogeomorphic state variables and phasespace construction for quantifying the evolution of vegetated aeolian landscapes, *Earth Surface Processes and Landforms*, 35, 717–731, <https://doi.org/10.1002/esp.1990>, 2010.
- 720 Bakker, J.: Ecology of salt marshes: 40 years of research in the Wadden Sea, Wadden Academy, Leeuwarden, ISBN 9789490289324, 2014.
- Barbier, E. B., Hacker, S. D., Kennedy, C., Koch, E. W., Stier, A. C., and Silliman, B. R.: The value of estuarine and coastal ecosystem services, *Ecological monographs*, 81, 169–193, 2011.
- Biel, R. G. and Hacker, S. D.: Climate Change Alters The Interaction of Two Invasive Beachgrasses With Implications For Range Shifts And Coastal Dune Functions, <https://doi.org/10.21203/rs.3.rs-529207/v1>, 2021.
- 725 Biel, R. G., Hacker, S. D., and Ruggiero, P.: Elucidating Coastal Foredune Ecomorphodynamics in the U.S. Pacific Northwest via Bayesian Networks, *Journal of Geophysical Research: Earth Surface*, 124, 1919–1938, <https://doi.org/10.1029/2018JF004758>, 2019.
- Bonte, D., Batsleer, F., Provoost, S., Reijers, V., Vandegehuchte, M. L., van de Walle, R., Dan, S., Matheve, H., Rauwoens, P., Strypsteen, G., Suzuki, T., Verwaest, T., and Hillaert, J.: Biomorphogenic feedbacks and the spatial organisation of a dominant grass steer dune development, *Frontiers in Ecology and Evolution*, 11, <https://doi.org/10.3389/fevo.2021.761336>, 2021.
- 730 Boorman, L. A.: The grazing management of sand dunes: Handbook: (Unpublished), 1988.
- Bouma, T. J., Temmerman, S., van Duren, L. A., Martini, E., Vandenbruwaene, W., Callaghan, D. P., Balke, T., Biermans, G., Klaassen, P. C., van Steeg, P., Dekker, F., van de Koppel, J., de Vries, M. B., and Herman, P.: Organism traits determine the strength of scale-dependent bio-geomorphic feedbacks: A flume study on three intertidal plant species, *Geomorphology*, 180-181, 57–65, <https://doi.org/10.1016/j.geomorph.2012.09.005>, 2013.
- 735 Bressolier, C. and Thomas, Y.-F.: Studies on Wind and Plant Interactions on French Atlantic Coastal Dunes, *Journal of Sedimentary Petrology*, 47, 331–338, 1977.
- Bryant, D. B., Anderson Bryant, M., Sharp, J. A., Bell, G. L., and Moore, C.: The response of vegetated dunes to wave attack, *Coastal Engineering*, 152, 103–106, <https://doi.org/10.1016/j.coastaleng.2019.103506>, 2019.
- Carter, R. W. G.: Near-future sea level impacts on coastal dune landscapes, *Landscape Ecology*, 6, 29–39, <https://doi.org/10.1007/BF00157742>, 1991.
- 740 Chergui, A., El Hafid, L., and Melhaoui, M.: Characteristics of marram grass (*Ammophila arenaria* L.), plant of the coastal dunes of the Mediterranean Eastern Morocco: Ecological, morpho-anatomical and physiological aspects, *Journal of Materials and Environmental Sciences*, 8, 3759–3765, 2017.
- Costas, S., Sousa, L. B. d., Gallego-Fernández, J. B., Hesp, P., and Kombiadou, K.: Foredune initiation and early development through biophysical interactions, *Science of The Total Environment*, p. 173548, <https://doi.org/10.1016/j.scitotenv.2024.173548>, 2024.
- 745 Dangendorf, S., Hay, C., Calafat, F. M., Marcos, M., Piecuch, C. G., Berk, K., and Jensen, J.: Persistent acceleration in global sea-level rise since the 1960s, *Nature Climate Change*, 9, 705–710, <https://doi.org/10.1038/s41558-019-0531-8>, 2019.
- Davidson, S. G., Hesp, P. A., and Da Silva, G. M.: Controls on dune scarping, *Progress in Physical Geography*, 44, 923–947, <https://doi.org/10.1177/0309133320932880>, 2020.
- 750 Davis, J. H.: Dune formation and stabilization by vegetation and plantings, *Coastal Engineering Proceedings*, 1, 29, <https://doi.org/10.9753/icce.v6.29>, 2011.



- de Battisti, D.: The resilience of coastal ecosystems: A functional trait-based perspective, *Journal of Ecology*, 109, 3133–3146, <https://doi.org/10.1111/1365-2745.13641>, 2021.
- 755 de Battisti, D. and Griffin, J. N.: Below-ground biomass of plants, with a key contribution of buried shoots, increases foredune resistance to wave swash, *Annals of Botany*, 125, 325–334, <https://doi.org/10.1093/aob/mcz125>, 2020.
- de Jong, B., Keijsers, J. G. S., Riksen, M. J. P. M., Krol, J., and Slim, P. A.: Soft engineering vs a dynamic approach in coastal dune management: A case study on the North Sea Barrier Island of Ameland, The Netherlands, *Journal of Coastal Research*, 30, 670–684, <https://doi.org/10.2112/JCOASTRES-D-13-00125.1>, 2014.
- de Vries, S., Southgate, H. N., Kanning, W., and Ranasinghe, R.: Dune behavior and aeolian transport on decadal timescales, *Coastal Engineering*, 67, 41–53, <https://doi.org/10.1016/j.coastaleng.2012.04.002>, 2012.
- 760 Deutscher Wetterdienst: 10-minute station observations of wind for Germany, https://opendata.dwd.de/climate_environment/CDC/observations_germany/climate/10_minutes/wind/historical/.
- Döring, M., Walsh, C., and Egberts, L.: “Beyond nature and culture: relational perspectives on the Wadden Sea landscape”, *Maritime Studies*, 20, 225–234, <https://doi.org/10.1007/s40152-021-00246-x>, 2021.
- 765 Du, F. and Jiao, Y.: Mechanical control of plant morphogenesis: concepts and progress, *Current opinion in plant biology*, 57, 16–23, <https://doi.org/10.1016/j.pbi.2020.05.008>, 2020.
- Duarte, C. M., Losada, I. J., Hendriks, I. E., Mazarrasa, I., and Marbà, N.: The role of coastal plant communities for climate change mitigation and adaptation, *Nature Climate Change*, 3, 961–968, <https://doi.org/10.1038/nclimate1970>, 2013.
- Everard, M., Jones, L., and Watts, B.: Have we neglected the societal importance of sand dunes? An ecosystem services perspective, *Aquatic Conservation: Marine and Freshwater Ecosystems*, 20, 476–487, <https://doi.org/10.1002/aqc.1114>, 2010.
- 770 Farrell, E. J., Delgado Fernandez, I., Smyth, T., Li, B., and Swann, C.: Contemporary research in coastal dunes and aeolian processes, *Earth Surface Processes and Landforms*, <https://doi.org/10.1002/esp.5597>, 2023.
- Feagin, R. A., Figlus, J., Zinnert, J. C., Sigren, J., Martínez, M. L., Silva, R., Smith, W. K., Cox, D., Young, D. R., and Carter, G.: Going with the flow or against the grain? The promise of vegetation for protecting beaches, dunes, and barrier islands from erosion, *Frontiers in Ecology and the Environment*, 13, 203–210, <https://doi.org/10.1890/140218>, 2015.
- 775 Feagin, R. A., Furman, M., Salgado, K., Martinez, M. L., Innocenti, R. A., Eubanks, K., Figlus, J., Huff, T. P., Sigren, J., and Silva, R.: The role of beach and sand dune vegetation in mediating wave run up erosion, *Estuarine, Coastal and Shelf Science*, 219, 97–106, <https://doi.org/10.1016/j.ecss.2019.01.018>, 2019.
- Figlus, J.: Designing and implementing coastal dunes for flood risk reduction, in: *Coastal Flood Risk Reduction*, pp. 287–301, Elsevier, ISBN 9780323852517, <https://doi.org/10.1016/B978-0-323-85251-7.00021-4>, 2022.
- 780 Figlus, J., Kobayashi, N., Gralher, C., and Iranzo, V.: Wave Overtopping and Overwash of Dunes, *Journal of Waterway, Port, Coastal, and Ocean Engineering*, 137, 26–33, [https://doi.org/10.1061/\(ASCE\)WW.1943-5460.0000060](https://doi.org/10.1061/(ASCE)WW.1943-5460.0000060), 2011.
- Figlus, J., Sigren, J. M., Armitage, A. R., and Tyler, R. C.: Erosion of vegetated coastal dunes, *Coastal Engineering Proceedings*, 1, 20, <https://doi.org/10.9753/icce.v34.sediment.20>, 2014.
- 785 Foster-Martinez, M. R., Lacy, J. R., Ferner, M. C., and Variano, E. A.: Wave attenuation across a tidal marsh in San Francisco Bay, *Coastal Engineering*, 136, 26–40, <https://doi.org/10.1016/j.coastaleng.2018.02.001>, 2018.
- Freschet, G. T. and Roumet, C.: Sampling roots to capture plant and soil functions, *Functional Ecology*, 31, 1506–1518, <https://doi.org/10.1111/1365-2435.12883>, 2017.



- Gao, J., Kennedy, D. M., and Konlechner, T. M.: Coastal dune mobility over the past century: A global review, *Progress in Physical Geography: Earth and Environment*, 44, 814–836, <https://doi.org/10.1177/0309133320919612>, 2020.
- 790 Gardiner, B., Berry, P., and Moulia, B.: Review: Wind impacts on plant growth, mechanics and damage, *Plant science : an international journal of experimental plant biology*, 245, 94–118, <https://doi.org/10.1016/j.plantsci.2016.01.006>, 2016.
- Garzon, J. L., Costas, S., and Ferreira, O.: Biotic and abiotic factors governing dune response to storm events, *Earth Surface Processes and Landforms*, <https://doi.org/10.1002/esp.5300>, 2021.
- 795 GDWS: Pegel online: Spiekeroog: 9410010, 1, <https://www.pegelonline.wsv.de/gast/stammdaten?pegelnr=9410010>, 2024.
- González-Villanueva, R., Pastoriza, M., Hernández, A., Carballeira, R., Sáez, A., and Bao, R.: Primary drivers of dune cover and shoreline dynamics: A conceptual model based on the Iberian Atlantic coast, *Geomorphology*, 423, 108556, <https://doi.org/10.1016/j.geomorph.2022.108556>, 2023.
- Gracia, A., Rangel-Buitrago, N., Oakley, J. A., and Williams, A. T.: Use of ecosystems in coastal erosion management, *Ocean & Coastal*
800 *Management*, 156, 277–289, <https://doi.org/10.1016/j.ocecoaman.2017.07.009>, 2018.
- Hacker, S. D., Zarnetske, P., Seabloom, E., Ruggiero, P., Mull, J., Gerrity, S., and Jones, C.: Subtle differences in two non-native congeneric beach grasses significantly affect their colonization, spread, and impact, *Oikos*, 121, 138–148, <https://doi.org/10.1111/j.1600-0706.2011.18887.x>, 2012.
- Hesp, P.: Foredunes and blowouts: initiation, geomorphology and dynamics, *Geomorphology*, 48, 245–268, [https://doi.org/10.1016/S0169-555X\(02\)00184-8](https://doi.org/10.1016/S0169-555X(02)00184-8), 2002.
- 805 Hesp, P. A.: The Formation of Shadow Dunes, *Journal of Sedimentary Petrology*, 51, 101–112, 1981.
- Hesp, P. A.: A review of biological and geomorphological processes involved in the initiation and development of incipient foredunes, *Proceedings of the Royal Society of Edinburgh*, 96b, 181–201, <https://doi.org/10.1017/S0269727000010927>, 1989.
- Hild, A., Niesel, V., and Günther, C.-P.: Study Area: The Backbarrier Tidal Flats of Spiekeroog, in: *The Wadden Sea Ecosystem*, edited by
810 Dittmann, S., pp. 15–49, Springer Berlin Heidelberg, Berlin, Heidelberg, ISBN 978-3-642-64256-2, https://doi.org/10.1007/978-3-642-60097-5_3, 1999.
- Hovenga, P. A., Ruggiero, P., Goldstein, E. B., Hacker, S. D., and Moore, L. J.: The relative role of constructive and destructive processes in dune evolution on Cape Lookout National Seashore, North Carolina, USA, *Earth Surface Processes and Landforms*, 46, 2824–2840, <https://doi.org/10.1002/esp.5210>, 2021.
- 815 Huiskes, A. H. L.: Biological Flora of the British isles: *Ammophila arenaria* (L.) Link (*Psamma Arenaria* (L.) Roem. et Schult.; *Calamagrostis Arenaria* (L.) Roth), *Journal of Ecology*, 67, 363, <https://doi.org/10.2307/2259356>, 1979.
- Husemann, P., Romão, F., Lima, M., Costas, S., and Coelho, C.: Review of the Quantification of Aeolian Sediment Transport in Coastal Areas, *Journal of Marine Science and Engineering*, 12, 2024.
- Isermann, M.: Patterns in Species Diversity during Succession of Coastal Dunes, *Journal of Coastal Research*, 27, 661–671, 2011.
- 820 Isermann, M. and Cordes, H.: Changes in dune vegetation on Spiekeroog (East Friesian islands) over a 30 year period, in: *Coastal Dunes: Geomorphology, Ecology and Management for Conservation.*, edited by Carter, R., Curtis, T., and Sheehy-Skeffington, M. J., pp. 201–209, Balkema, Rotterdam, 1997.
- Keijsers, J., de Groot, A. V., and Riksen, M.: Modeling the biogeomorphic evolution of coastal dunes in response to climate change, *Journal of Geophysical Research: Earth Surface*, 121, 1161–1181, <https://doi.org/10.1002/2015JF003815>, 2016.



- 825 Keijsers, J. G. S., Giardino, A., Poortinga, A., Mulder, J. P. M., Riksen, M. J. P. M., and Santinelli, G.: Adaptation strategies to maintain dunes as flexible coastal flood defense in The Netherlands, *Mitigation and Adaptation Strategies for Global Change*, 20, 913–928, <https://doi.org/10.1007/s11027-014-9579-y>, 2015.
- Keimer, K., Kosmalla, V., Prüter, I., Lojek, O., Prinz, M., Schürenkamp, D., Freund, H., and Goseberg, N.: Proposing a novel classification of growth periods based on biomechanical properties and seasonal changes of *Spartina anglica*, *Frontiers in Marine Science*, 10, <https://doi.org/10.3389/fmars.2023.1095200>, 2023.
- 830 Keimer, K., Kind, F., Prüter, I., Kosmalla, V., Lojek, O., Schürenkamp, D., Prinz, M., Niewerth, S., Aberle, J., and Goseberg, N.: From seasonal field study to surrogate modeling: Investigating the biomechanical dynamics of *Elymus sp.* in salt marshes, *Limnology and Oceanography: Methods*, <https://doi.org/10.1002/lom3.10616>, 2024.
- Kobayashi, N., Gralher, C., and Do, K.: Effects of Woody Plants on Dune Erosion and Overwash, *Journal of Waterway, Port, Coastal, and Ocean Engineering*, 139, 466–472, [https://doi.org/10.1061/\(ASCE\)WW.1943-5460.0000200](https://doi.org/10.1061/(ASCE)WW.1943-5460.0000200), 2013.
- 835 Koch, E. W., Barbier, E. B., Silliman, B. R., Reed, D. J., Perillo, G. M. E., Hacker, S. D., Granek, E. F., Primavera, J. H., Muthiga, N., Polasky, S., Halpern, B. S., Kennedy, C. J., Kappel, C. V., and Wolanski, E.: Non-linearity in ecosystem services: temporal and spatial variability in coastal protection, *Frontiers in Ecology and the Environment*, 7, 29–37, <https://doi.org/10.1890/080126>, 2009.
- Konlechner, T. M. and Hilton, M. J.: Post-disturbance evolution of a prograded foredune barrier during a sustained dynamic restoration project—the role of wind speed, wind direction and vegetation, *Earth Surface Processes and Landforms*, 47, 3435–3452, <https://doi.org/10.1002/esp.5466>, 2022.
- 840 Kosmalla, V., Lojek, O., Ahrenbeck, L., Mehrtens, B., Schürenkamp, D., and Goseberg, N.: Towards accurate modeling of aboveground vegetation in white dunes: biomechanics of marram grass (*Ammophila arenaria*), *CoastLab 2024: Physical Modelling in Coastal Engineering and Science*, <https://doi.org/10.59490/coastlab.2024.798>, 2024.
- 845 Kouhen, M., Dimitrova, A., Scippa, G. S., and Trupiano, D.: The Course of Mechanical Stress: Types, Perception, and Plant Response, *Biology*, 12, <https://doi.org/10.3390/biology12020217>, 2023.
- LGLN: Digitales Orthophoto (DOP20) [Digital orthophotos]: Landesamt für Geoinformationen und Landesvermessung Niedersachsen [State agency for geoinformation and state survey of Lower Saxony]: Data licence Germany – attribution – Version 2.0, ATKIS, 1, <https://ni-igl-n-opengeodata.hub.arcgis.com/apps/igl-n-opengeodata::digitales-orthophoto-dop20/about>, 2024.
- 850 Li, C., Peng, Z., Zhao, Y., Fang, D., Chen, X., Xu, F., and Wang, X.: Seasonal variations in drag coefficient of salt marsh vegetation, *Coastal Engineering*, 193, 104 575, <https://doi.org/10.1016/j.coastaleng.2024.104575>, 2024.
- Liu, J., Kutschke, S., Keimer, K., Kosmalla, V., Schürenkamp, D., Goseberg, N., and Böhl, M.: Experimental characterisation and three-dimensional modelling of *Elymus* for the assessment of ecosystem services, *Ecological Engineering*, 166, <https://doi.org/10.1016/j.ecoleng.2021.106233>, 2021.
- 855 Martínez, M. L. and Psuty, N. P.: Coastal Dunes: Ecology and Conservation, vol. 171 of *Ecological Studies*, Springer Berlin / Heidelberg, ISBN 9783540740025, 2004.
- Maun, M. A.: Adaptations of plants to burial in coastal sand dunes, *Canadian Journal of Botany*, 76, 713–738, <https://doi.org/10.1139/b98-058>, 1998.
- Maximiliano-Cordova, C., Salgado, K., Martínez, M. L., Mendoza, E., Silva, R., Guevara, R., and Feagin, R. A.: Does the Functional Richness of Plants Reduce Wave Erosion on Embryo Coastal Dunes?, *Estuaries and Coasts*, 42, 1730–1741, <https://doi.org/10.1007/s12237-019-00537-x>, 2019.
- 860



- McGuirk, M. T., Kennedy, D. M., and Konlechner, T.: The Role of Vegetation in Incipient Dune and Fore-dune Development and Morphology: A Review, *Journal of Coastal Research*, 38, <https://doi.org/10.2112/JCOASTRES-D-21-00021.1>, 2022.
- 865 Mehrtens, B., Kosmalla, V., Bölker, T., Lojek, O., and Goseberg, N.: Spatial and temporal growth of coastal dune - field observation of the German Wadden Sea Coast, in: *Book of abstracts: Building Coastal Resilience 2022*, edited by Strypsteen, Glenn, G., Roest, Bart, B., and Rauwoens, Pieter, P., VLIZ Special Publication, <https://doi.org/10.48470/28>, 2022.
- Mehrtens, B., Lojek, O., Kosmalla, V., Bölker, T., and Goseberg, N.: Fore-dune growth and storm surge protection potential at the Eiderstedt Peninsula, Germany, *Frontiers in Marine Science*, 9, <https://doi.org/10.3389/fmars.2022.1020351>, 2023.
- 870 Mehrtens, B., Lojek, O., Bölker, T., Ahrenbeck, L., Kosmalla, V., Schweiger, C., Schürenkamp, D., and Goseberg, N.: Experimental Investigation Of Coastal Fore-dune Erosion, *CoastLab 2024: Physical Modelling in Coastal Engineering and Science*, <https://doi.org/10.59490/coastlab.2024.794>, 2024.
- Montreuil, A.-L., Bullard, J. E., Chandler, J. H., and Millett, J.: Decadal and seasonal development of embryo dunes on an accreting macrotidal beach: North Lincolnshire, UK, *Earth Surface Processes and Landforms*, 38, 1851–1868, <https://doi.org/10.1002/esp.3432>, 2013.
- 875 Mostow, R. S., Barreto, F., Biel, R. G., Meyer, E., and Hacker, S. D.: Discovery of a dune-building hybrid beachgrass (*Ammophila arenaria* × *A. breviligulata*) in the U.S. Pacific Northwest, *Ecosphere*, 12, <https://doi.org/10.1002/ecs2.3501>, 2021.
- NLWKN: 80.000 Kubikmeter Sand sollen Spiekeroog schützen, https://www.nlwkn.niedersachsen.de/startseite/aktuelles/presse_und_offentlichkeitsarbeit/pressemitteilungen/80-000-kubikmeter-sand-sollen-spiekeroog-schutzen-223919.html, 14.07.2023.
- NLWKN: Digital Elevation Model Spiekeroog: Forschungsstelle Küste, airborne topography survey, 2023, 2023.
- 880 Paul, M., Bischoff, C., and Koop-Jakobsen, K.: Biomechanical traits of salt marsh vegetation are insensitive to future climate scenarios, *Scientific Reports*, 12, 21 272, <https://doi.org/10.1038/s41598-022-25525-3>, 2022.
- Pickart, A. J.: *Ammophila* invasion ecology and dune restoration on the west coast of North America, *Diversity*, 13, 629, <https://doi.org/10.3390/d13120629>, 2021.
- Pollmann, T., Junge, B., and Giani, L.: Landscapes and soils of North Sea barrier islands: A comparative analysis of the old west and young east of Spiekeroog island (Germany), *Erdkunde*, 72, 273–286, 2018.
- 885 Pott, R.: *Die Pflanzengesellschaften Deutschlands*, vol. 8067 of *UTB für Wissenschaft Große Reihe Botanik, Ökologie, Agrar- und Forstwissenschaften*, Ulmer, Stuttgart, 2., überarb. und stark erw. Aufl. edn., ISBN 9783825280673, 1995.
- Puijalon, S., Bornette, G., and Sagnes, P.: Adaptations to increasing hydraulic stress: morphology, hydrodynamics and fitness of two higher aquatic plant species, *Journal of Experimental Botany*, 56, 777–786, <https://doi.org/10.1093/jxb/eri063>, 2005.
- Puijalon, S., Bouma, T. J., Douady, C. J., van Groenendael, J., Anten, N., Martel, E., and Bornette, G.: Plant resistance to mechanical stress: 890 evidence of an avoidance-tolerance trade-off, *New Phytologist*, 191, 1141–1149, <https://doi.org/10.1111/j.1469-8137.2011.03763.x>, 2011.
- Pye, K. and Blott, S. J.: Assessment of beach and dune erosion and accretion using LiDAR: Impact of the stormy 2013–14 winter and longer term trends on the Sefton Coast, UK, *Geomorphology*, 266, 146–167, <https://doi.org/10.1016/j.geomorph.2016.05.011>, 2016.
- Rader, A. M., Pickart, A. J., Walker, I. J., Hesp, P. A., and Bauer, B. O.: Fore-dune morphodynamics and sediment budgets at seasonal to decadal scales: Humboldt Bay National Wildlife Refuge, California, USA, *Geomorphology*, 318, 69–87, 895 <https://doi.org/10.1016/j.geomorph.2018.06.003>, 2018.
- Röper, T., Greskowiak, J., Freund, H., and Massmann, G.: Freshwater lens formation below juvenile dunes on a barrier island (Spiekeroog, Northwest Germany), *Estuarine, Coastal and Shelf Science*, 121–122, 40–50, <https://doi.org/10.1016/j.ecss.2013.02.004>, 2013.
- Ruggiero, P., Hacker, S., Seabloom, E., and Zarnetske, P.: The Role of Vegetation in Determining Dune Morphology, Exposure to Sea-Level Rise, and Storm-Induced Coastal Hazards: A U.S. Pacific Northwest Perspective, in: *Barrier Dynamics and Response to Changing*



- 900 Climate, edited by Moore, L. J. and Murray, A. B., pp. 337–361, Springer International Publishing, Cham, ISBN 978-3-319-68084-2, https://doi.org/10.1007/978-3-319-68086-6_11, 2018.
- Rupprecht, F., Möller, I., Evans, B., Spencer, T., and Jensen, K.: Biophysical properties of salt marsh canopies - Quantifying plant stem flexibility and above ground biomass, *Coastal Engineering*, 100, 48–57, <https://doi.org/10.1016/j.coastaleng.2015.03.009>, 2015.
- Rupprecht, F., Möller, I., Paul, M., Kudella, M., Spencer, T., van Wesenbeeck, B. K., Wolters, G., Jensen, K., Bouma, T. J., Miranda-Lange,
905 M., and Schimmels, S.: Vegetation-wave interactions in salt marshes under storm surge conditions, *Ecological Engineering*, 100, 301–315, <https://doi.org/10.1016/j.ecoleng.2016.12.030>, 2017.
- Scantronik Mugrauer GmbH: Data sheet for: Soil Analysis Sensor (Digital) + Analog Soil Sensor, Revision 2.0, <https://www.scantronik.de/English/Soil%20Sensor%20-%20Datasheet.pdf>, 2024a.
- Scantronik Mugrauer GmbH: Thermofox and Hygrofox: Operating instructions, [https://www.scantronik.de/English/Manual%20for%
910 20the%20Hygrofox%20and%20Thermofox%20Universal.pdf](https://www.scantronik.de/English/Manual%20for%20the%20Hygrofox%20and%20Thermofox%20Universal.pdf), 2024b.
- Schweiger, C. and Schuettrumpf, H.: Considering the Effect of Land-Based Biomass on Dune Erosion Volumes in Large-Scale Numerical Modeling, *Journal of Marine Science and Engineering*, 9, 843, <https://doi.org/10.3390/jmse9080843>, 2021.
- Seabloom, E. W. and Wiedemann, A. M.: Distribution and effects of *Ammophila breviligulata* Fern. (American Beachgrass) on the foredunes of the Washington coast, *Journal of Coastal Research*, 10, 178–188, 1994.
- 915 Silva, R., Martínez, M. L., Odériz, I., Mendoza, E., and Feagin, R. A.: Response of vegetated dune–beach systems to storm conditions, *Coastal Engineering*, 109, 53–62, <https://doi.org/10.1016/j.coastaleng.2015.12.007>, 2016.
- Staudt, F., Gijssman, R., Ganal, C., Mielck, F., Wolbring, J., Hass, H. C., Goseberg, N., Schüttrumpf, H., Schlurmann, T., and Schimmels, S.: The sustainability of beach nourishments: a review of nourishment and environmental monitoring practice, *Journal of Coastal Conservation*, 25, 1–24, <https://doi.org/10.1007/s11852-021-00801-y>, 2021.
- 920 Strypsteen, G., Houthuys, R., and Rauwoens, P.: Dune Volume Changes at Decadal Timescales and Its Relation with Potential Aeolian Transport, *Journal of Marine Science and Engineering*, 7, 357, <https://doi.org/10.3390/jmse7100357>, 2019.
- Strypsteen, G., Delgado-Fernandez, I., Derijckere, J., and Rauwoens, P.: Fetch–driven aeolian sediment transport on a sandy beach: A new study, *Earth Surface Processes and Landforms*, <https://doi.org/10.1002/esp.5784>, 2024.
- Telewski, F. W.: Thigmomorphogenesis: the response of plants to mechanical perturbation, *Italus Hortus*, 23, 1–16, 2016.
- 925 Tomasicchio, G. R., Sánchez-Arcilla, A., D’Alessandro, F., Ilic, S., James, M. R., Sancho, F., Fortes, C. J., and Schüttrumpf, H.: Large-scale experiments on dune erosion processes, *Journal of Hydraulic Research*, 49, 20–30, <https://doi.org/10.1080/00221686.2011.604574>, 2011.
- Türker, U., Yagci, O., and Kaldasli, M. S.: Impact of nearshore vegetation on coastal dune erosion: assessment through laboratory experiments, *Environmental Earth Sciences*, 78, <https://doi.org/10.1007/s12665-019-8602-8>, 2019.
- van der Putten, W. H. and Troelstra, S. R.: Harmful soil organisms in coastal foredunes involved in degeneration of *Ammophila arenaria* and
930 *Calammophila baltica*, *Canadian Journal of Botany*, 68, 1560–1568, 1990.
- van Gent, M. R. A., Coeveld, E. M., de Vroeg, H., and van de Graaff, J.: Dune erosion prediction methods incorporating effects of wave periods, *Coastal Sediments 2007 Conference Paper*, pp. 612–625, [https://doi.org/10.1061/40926\(239\)46](https://doi.org/10.1061/40926(239)46), 2007.
- van Gent, M. R. A., van Thiel de Vries, J., Coeveld, E. M., de Vroeg, J. H., and van de Graaff, J.: Large-scale dune erosion tests to study the influence of wave periods, *Coastal Engineering*, 55, 1041–1051, <https://doi.org/10.1016/j.coastaleng.2008.04.003>, 2008.
- 935 van IJendoorn, C. O., de Vries, S., Hallin, C., and Hesp, P. A.: Sea level rise outpaced by vertical dune toe translation on prograding coasts, *Scientific Reports*, 11, 12 792, <https://doi.org/10.1038/s41598-021-92150-x>, 2021.



- van Westen, B., de Vries, S., Cohn, N., van IJzendoorn, C., Strypsteen, G., and Hallin, C.: AeoliS: Numerical modelling of coastal dunes and aeolian landform development for real-world applications, *Environmental Modelling & Software*, 179, 106093, <https://doi.org/10.1016/j.envsoft.2024.106093>, 2024.
- 940 Vuik, V., Suh Heo, H. Y., Zhu, Z., Borsje, B. W., and Jonkman, S. N.: Stem breakage of salt marsh vegetation under wave forcing: A field and model study, *Estuarine, Coastal and Shelf Science*, 200, 41–58, <https://doi.org/10.1016/j.ecss.2017.09.028>, 2017.
- Walker, S. L. and Zinnert, J.: Whole plant traits of coastal dune vegetation and implications for interactions with dune dynamics, *Ecosphere*, 13, <https://doi.org/10.1002/ecs2.4065>, 2022.
- Zarnetske, P. L., Hacker, S. D., Seabloom, E. W., Ruggiero, P., Killian, J. R., Maddux, T. B., and Cox, D.: Biophysical feedback mediates effects of invasive grasses on coastal dune shape, *Ecology*, 93, 1439–1450, <https://doi.org/10.1890/11-1112.1>, 2012.
- 945 Zarnetske, P. L., Ruggiero, P., Seabloom, E. W., and Hacker, S. D.: Coastal foredune evolution: the relative influence of vegetation and sand supply in the US Pacific Northwest, *Journal of the Royal Society, Interface*, 12, <https://doi.org/10.1098/rsif.2015.0017>, 2015.
- Zhu, Z., Yang, Z., and Bouma, T. J.: Biomechanical properties of marsh vegetation in space and time: effects of salinity, inundation and seasonality, *Annals of Botany*, 125, 277–290, <https://doi.org/10.1093/aob/mcz063>, 2020.
- 950 ZwickRoell GmbH & Co.KG: Product Information: Materials Testing Machines zwickiLine Z0.5 to Z5.0, https://www.zwickroell.com/fileadmin/content/Files/SharePoint/user_upload/PI_EN/02_396_zwickiLine_Z0_5_up_to_Z5_0_Materials_Testing_Machine_PI_EN.pdf, 2024.